NBS SPECIAL PUBLICATION 400-59

U.S. DEPARTMENT OF COMMERCE/National Bureau of Standards

Semiconductor Measurement Technology:

Nondestructive Tests Used to Insure the Integrity of Semiconductor Devices, with Emphasis on Acoustic Emission Techniques

NATIONAL BUREAU OF STANDARDS

The National Bureau of Standards[1] was established by an act of Congress on March 3, 1901. The Bureau's overall goal is to strengthen and advance the Nation's science and technology and facilitate their effective application for public benefit. To this end, the Bureau conducts research and provides: (1) a basis for the Nation's physical measurement system, (2) scientific and technological services for industry and government, (3) a technical basis for equity in trade, and (4) technical services to promote public safety. The Bureau's technical work is performed by the National Measurement Laboratory, the National Engineering Laboratory, and the Institute for Computer Sciences and Technology.

THE NATIONAL MEASUREMENT LABORATORY provides the national system of physical and chemical and materials measurement; coordinates the system with measurement systems of other nations and furnishes essential services leading to accurate and uniform physical and chemical measurement throughout the Nation's scientific community, industry, and commerce; conducts materials research leading to improved methods of measurement, standards, and data on the properties of materials needed by industry, commerce, educational institutions, and Government; provides advisory and research services to other Government agencies; develops, produces, and distributes Standard Reference Materials; and provides calibration services. The Laboratory consists of the following centers:

Absolute Physical Quantities[2] — Radiation Research — Thermodynamics and Molecular Science — Analytical Chemistry — Materials Science.

THE NATIONAL ENGINEERING LABORATORY provides technology and technical services to the public and private sectors to address national needs and to solve national problems; conducts research in engineering and applied science in support of these efforts; builds and maintains competence in the necessary disciplines required to carry out this research and technical service; develops engineering data and measurement capabilities; provides engineering measurement traceability services; develops test methods and proposes engineering standards and code changes; develops and proposes new engineering practices; and develops and improves mechanisms to transfer results of its research to the ultimate user. The Laboratory consists of the following centers:

Applied Mathematics — Electronics and Electrical Engineering[2] — Mechanical Engineering and Process Technology[2] — Building Technology — Fire Research — Consumer Product Technology — Field Methods.

THE INSTITUTE FOR COMPUTER SCIENCES AND TECHNOLOGY conducts research and provides scientific and technical services to aid Federal agencies in the selection, acquisition, application, and use of computer technology to improve effectiveness and economy in Government operations in accordance with Public Law 89-306 (40 U.S.C. 759), relevant Executive Orders, and other directives; carries out this mission by managing the Federal Information Processing Standards Program, developing Federal ADP standards guidelines, and managing Federal participation in ADP voluntary standardization activities; provides scientific and technological advisory services and assistance to Federal agencies; and provides the technical foundation for computer-related policies of the Federal Government. The Institute consists of the following centers:

Programming Science and Technology — Computer Systems Engineering.

[1]Headquarters and Laboratories at Gaithersburg, MD, unless otherwise noted; mailing address Washington, DC 20234.
[2]Some divisions within the center are located at Boulder, CO 80303.

Semiconductor Measurement Technology:

Nondestructive Tests Used to Insure the Integrity of Semiconductor Devices, with Emphasis on Acoustic Emission Techniques

George G. Harman

Center for Electronics and Electrical Engineering
National Engineering Laboratory
National Bureau of Standards
Washington, D.C. 20234

Sponsored in part by:
The Defense Advanced Research Projects Agency
1400 Wilson Boulevard
Arlington, VA 22209

U.S. DEPARTMENT OF COMMERCE, Juanita M. Kreps, Secretary
Luther H. Hodges, Jr., Under Secretary
Jordan J. Baruch, Assistant Secretary for Science and Technology
NATIONAL BUREAU OF STANDARDS, Ernest Ambler, Director

Issued September 1979

Library of Congress Catalog Card Number 79-600131

National Bureau of Standards Special Publication 400-59
Nat. Bur. Stand. (U.S.), Spec. Publ. 400-59, 72 pages (Sept. 1979)
CODEN: XNBSAV

U.S. GOVERNMENT PRINTING OFFICE
WASHINGTON: 1979

For sale by the Superintendent of Documents, U.S. Government Printing Office, Washington, D.C. 20402
Stock No. 003–003–02116–4 Price $3.50
(Add 25 percent additional for other than U.S. mailing).

☆ U.S. GOVERNMENT PRINTING OFFICE: 1979 O—300-303

Semiconductor Measurement Technology:
Nondestructive Tests Used to Insure the Integrity of Semiconductor Devices with Emphasis on Acoustic Emission Techniques

TABLE OF CONTENTS

Abstract v

1.1 Introduction 1

2.1 Some Current Production Line Assembly Tests 2

2.2 Introduction to Microelectronics and Hybrid Packaging Methods 2

2.3 Review of Typical Nondestructive Tests Used to Reveal Devices with Mechanical Defects 6

2.3.1 The Nondestructive Wire Bond Pull Test 6
2.3.2 Internal Visual Inspection 9
2.3.3 Temperature Cycling 9
2.3.4 Package Seal Leak Tests (Hermeticity) 11
2.3.4.1 Helium Mass Spectrometer Leak Detector Test 14
2.3.4.2 Bubble Emission Tests 15
2.3.5 Burn-In Test 16
2.3.6 Particle Impact Noise Detection (PIND) Test 19
2.3.7 The Statistics of Sampling for Special Production Lots 22

2.4 Conclusions of Section 2 23

3.1 Passive Acoustic Techniques 23

3.2 Introduction to Acoustic Emission 23

3.3 Review of Acoustic Emission Applications to the Real Time Nondestructive Testing of the Mechanical Integrity of Electronic Components 30

3.4 Acoustic Emission as a Post-Production Screen for Bond Integrity in Microelectronics 33

3.4.1 Introduction 33
3.4.2 Methods of Applying a Mechanical Stress to the Beam-Lead System 34
3.4.3 Preparation of Controlled Bondability Substrates . . 38
3.4.4 Experimental Apparatus 39
3.4.5 Experimental Results 46
3.4.5.1 AE Results from Pulling Beam Leaded Devices 46
3.4.5.2 Tests That Apply Force Only to the Beams . . 50

Page

3.4.6 Application of Acoustic Emission to Determine the Integrity of Tape Bonded Devices and Hybrid Components . 50

3.5 Conclusions of Section 3 61

Acknowledgment 62

References 62

ABSTRACT

The discussion is divided into two major sections. The first consists of an introduction to device assembly techniques and problems followed by a review of six important nondestructive tests used during and after device packaging to insure the mechanical integrity of completed electronic devices. Most of these tests are called out in the military testing standard, MIL-STD-883 and are generally classified as screens. The first section concludes with a brief introduction to the economic and other factors that result in the choice of one screen over another and to production line statistical sampling (LTPD) appropriate to special high reliability device lots such as those used for space flight.

The second section begins with an introduction to acoustic emission, the status of theory as it can be applied to microelectronics. Then the published papers that have applied AE as a nondestructive test in electronics applications will be reviewed. Finally, passive AE techniques are applied to establishing the mechanical bond integrity of beam lead, flip chip, and tape-bonded integrated circuits as well as components in hybrid microcircuits.

Key Words: Acoustic emission; beam lead devices; electronic devices; hermeticity; hybrids; nondestructive tests; semiconductor; tape-bonded devices.

Semiconductor Measurement Technology:
Nondestructive Tests Used to Insure the Integrity of Semiconductor Devices with Emphasis on Acoustic Emission Techniques

George G. Harman

Electron Devices Division
National Bureau of Standards
Washington, DC 20234

1.1 INTRODUCTION

This paper reviews a number of important nondestructive tests used frequently in the semiconductor industry to test the mechanical integrity of semiconductor devices. Many of these tests are not rigorously quantitative, but rather, involve an element of human judgment or some empirical comparison for interpretation. As such, the usage of some of the tests is controversial even though they are specified in important military and other microelectronic standards. The scientist or engineer just entering the microelectronics field should look upon this as an opportunity to develop better tests rather than be discouraged by the lack of rigor.

The discussion is divided into two major sections. The first section begins with a brief review of device assembly techniques and problems. This serves as necessary background for all of the material that follows. Next follows a review of six important nondestructive tests that are used during and after device packaging to insure the mechanical integrity of completed electronic devices. Most of these tests are called out in MIL-STD-883 [1], a widely used guide for device testing, and are generally classified as screens. These tests, presented in the order that they are usually performed are: (1) the nondestructive wire bond pull test, (2) internal visual inspection, (3) temperature cycling and shock, (4) package seal integrity (hermeticity), (5) burn-in (removing early failures), and (6) particle impact noise detection.

The first section concludes with a brief introduction to some factors that result in the choice of one screen over another and to production line statistical sampling appropriate to special high reliability device lots such as those used for space flight.

The second section begins with an introduction to acoustic emission (AE), and the status of its theory as it can be applied to microelectronics. Also, the published papers that have applied AE as a nondestructive test in electronics applications will be reviewed. Finally, acoustic emission measurement techniques developed at the NBS are applied to establishing the mechanical bond integrity of beam lead,

flip chip, and tape bonded integrated circuits as well as components in hybrid microcircuits.

2.1 SOME CURRENT PRODUCTION LINE ASSEMBLY TESTS

2.2 Introduction to Microelectronics and Hybrid Packaging Methods

Microelectronic assembly starts after the scribe-and-break or sawing operation that cuts the individual die (chips) from the wafer. Once cut out they are usually die-attached to the package by gold-silicon eutectic, a solder, or an epoxy and then conventionally interconnected by wire bonding. Other attach technologies, such as flip chip, beam-lead, and tape-carrier bonding can essentially combine die attach and interconnection bonding into a single operation. The first, most familiar, and still overwhelmingly dominant method of interconnection is to use flying wires, an example of which is shown in Figure 1. These wires, typically 25-μm diameter aluminum or gold, are welded on to the semiconductor bonding pads by thermocompression [2], ultrasonic [3], or thermosonic [4] (a combination of both) techniques.

The second method of interconnection uses gold beam leads, which are made during wafer processing, in place of wire bonds. Figure 2 is an example of such a device. These beams are welded to a package, usually a hybrid, by thermocompression techniques, in which the substrate is heated to $\sim 250^{\circ}C$ and a heated bonding tool compresses the leads against the substrate with forces > 100 kg/cm^2. The flip-chip approach requires building up the bonding pads, usually with a solder bump, and then reflow soldering the bumps to the package face down, obscuring the joints thus they cannot be visually inspected, discouraging the use of this technology. Several typical flip-chips are shown in Figure 3. Neither beam leads nor flip chips are used widely at present and their main applications are for large scale in-house production and consumption.

The final technique of interconnection which is relatively new is called tape bonding. For this, one normally builds up the semiconductor aluminum bonding pads into copper or gold "bumps" by plating techniques, then a special metallized tape with individual extended leads is bonded to the bumps by a thermocompression or reflow solder process. This is termed inner-lead bonding. Figure 4 gives two examples of chips bonded to such tape. The tape in 4A is "so called" testable tape. Here the individual insulated leads terminate on pads that may be probed and the device electrically tested after bonding. The tape in 4B is of all metal construction which cannot be tested before packaging. Once the chips are attached to the tape, it is usually wound onto reels and stored until final assembly into either an IC package or a hybrid. In the case of some calculators and watches, the leads are bonded onto a printed circuit board and the chip is protected by a drop of epoxy.

Figure 5 is a typical high technology thick film hybrid. In this figure, A is a chip capacitor, and B is a chip resistor. Some hybrids are very large (e.g., 5 × 10 cm) and the substrate may crack during

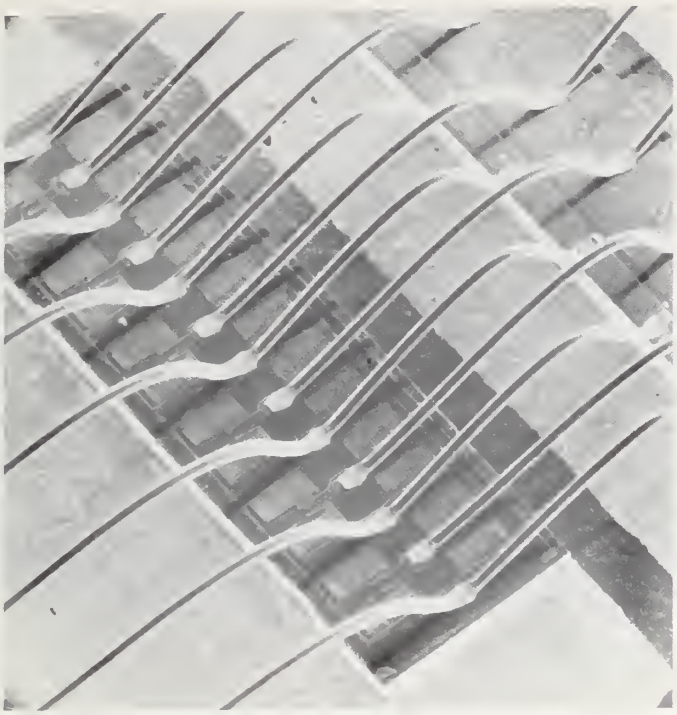

Figure 1. An example of 50-μm diameter aluminum ultrasonic wire bonds (flying wires) interconnecting a silicon microwave power transistor.

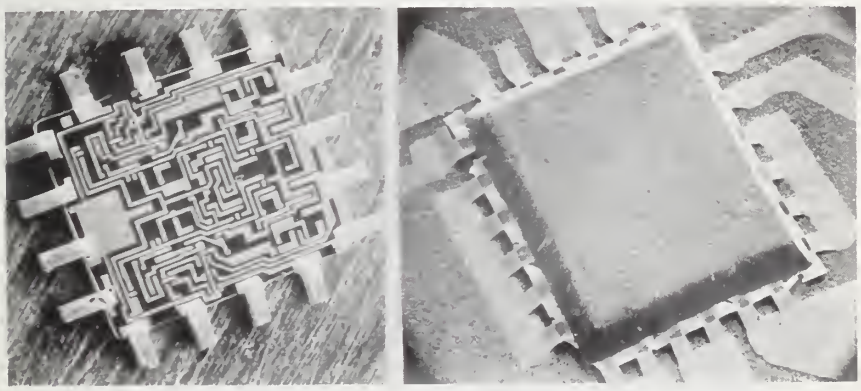

a b

Figure 2. (a) is a gold-beam lead device shown face up. Interconnections are made by the beams extending over the edge of the chip. (b) shows the device bonded into its hybrid microcircuit. The contact and metallization system is platinum silicide, titanium, platinum, and gold. The sealed junction is obtained by depositing silicon nitride over oxide layers.

a

b

Figure 3. (a) A solder bump flip-chip device shown soldered onto a substrate (b). Several devices shown face up. The solder bumps are apparent, covering what would be the bonding pads in a chip and wire device.

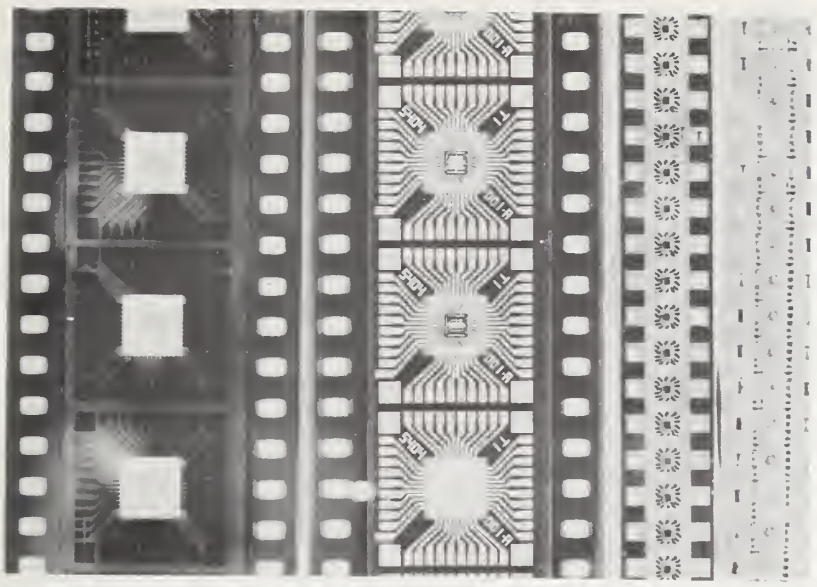

a b

Figure 4. (a) is a 35-mm, three-layer (metal, adhesive, polyamide) testable tape-bonded device. (b) is an example of an 11-mm copper all-metal single-layer tape with an IC chip inner-lead-bonded in the center. The leads are made of tin-plated copper. (Figs. 35, 38, and 39 give closeups of the bumped chips and bonded leads.)

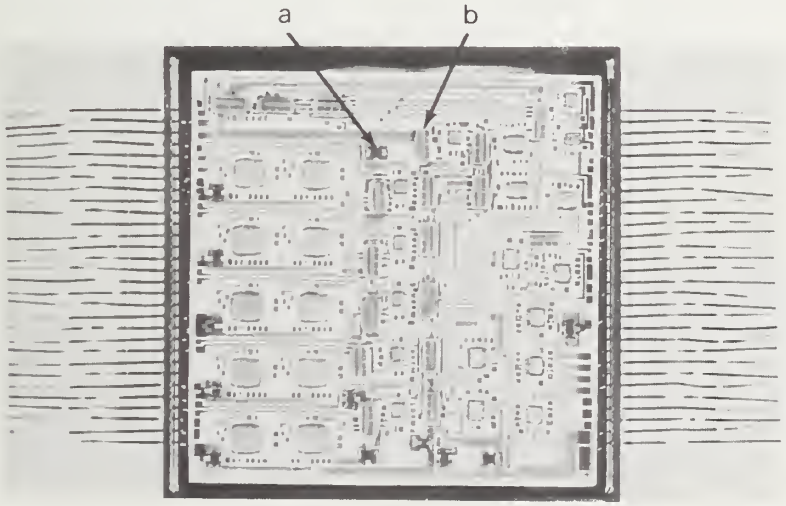

Figure 5. A high technology five-layer-thick film hybrid microcircuit. Arrows point to chip capacitors (a), and chip resistors (b). (Courtesy General Dynamics Electronics Division)

certain assembly operations such as thermocompression bonding. Some methods of detecting such cracks will be described in Section 3.3. Figure 6 is a photograph of such a large substrate. Once the hybrid components are assembled, the substrate is usually put in a package or epoxy coated. In the case of packages, there may be moisture leaks if the lid seal and metal leads are damaged or improperly assembled. The seal integrity of packages that contain numerous glass-to-metal lead-throughs is a potential reliability problem. Such seals are shown in Figure 7. Thomas [5] has stated that the glass seals are the major source of hermetic moisture ingress and that these may open only at high temperature and subsequently reseal, avoiding detection later in a normal leak test.

2.3 Review of Typical Nondestructive Tests Used to Reveal Devices with Mechanical Defects

There are a number of mechanical screens that may be applied to devices that have specific reliability requirements. The decision to implement one test over another can be based on such considerations as cost, the specifying engineers' personal familiarity with one test, or the availability of test personnel. It is therefore appropriate to briefly review the most common nondestructive tests used on assembly lines to verify mechanical integrity. These will be described in the order that they are usually performed on a production line.

2.3.1 The Nondestructive Wire Bond Pull Test

The purpose of the nondestructive wire bond pull test (NDPT) is to remove weak wire bonds having pull forces less than a designated force value, while avoiding damage to acceptable bonds. An example of a weak 25-μm diameter aluminum bond revealed by the NDPT is shown in Figure 8. This bond lifted at ∿ 0.2-grams force (gf). The bond would have passed any internal visual inspection (see 2.3.2) and its weakness could only be revealed by a pull test or possibly temperature cycling (2.3.3).

To perform the test, a hook, made of tungsten or steel wire, 2 to 3 times the diameter of the wire to be tested, is placed under the loop and a specified pull force is applied vertically to that loop. The bond and perhaps the device is rejected if the wire breaks. The pull force is usually specified for a given wire diameter, but it can also be derived from appropriate equations [6] based on the results of a sample destructive pull test and the metallurgical characteristics of the particular wire being tested. A typical equation is:

$$F = 0.9(\bar{X} - 3S_X)$$

where F is the nondestructive pull force (in gf), $\bar{X}$ and S_X are the mean and standard deviation of the destructive pull force respectively. This equation is appropriate for small diameter (25- to 50-μm) aluminum wire used for ultrasonic bonding.

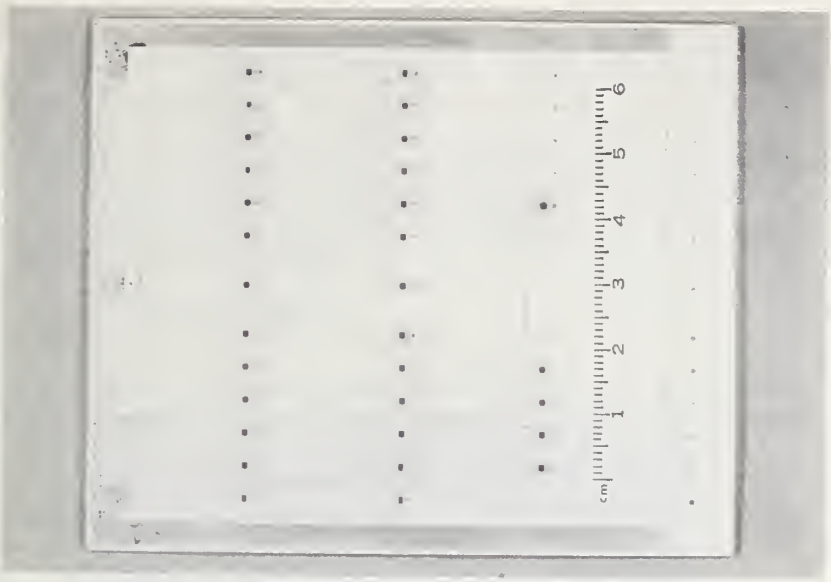

Figure 6. A large thin-film hybrid substrate. The ICs are beam lead devices bonded face down. The substrate is alumina ceramic and interconnection metallizations are titanium, palladium, and gold.

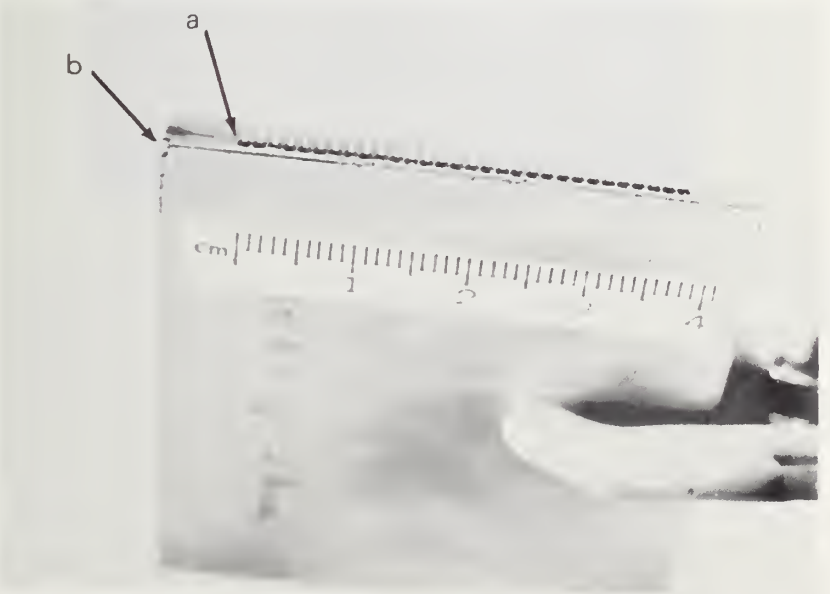

Figure 7. A 5 by 5 cm sealed hermetic-type hybrid package with numerous glass-metal seals (a). A gross leak in the package lid is also indicated (b).

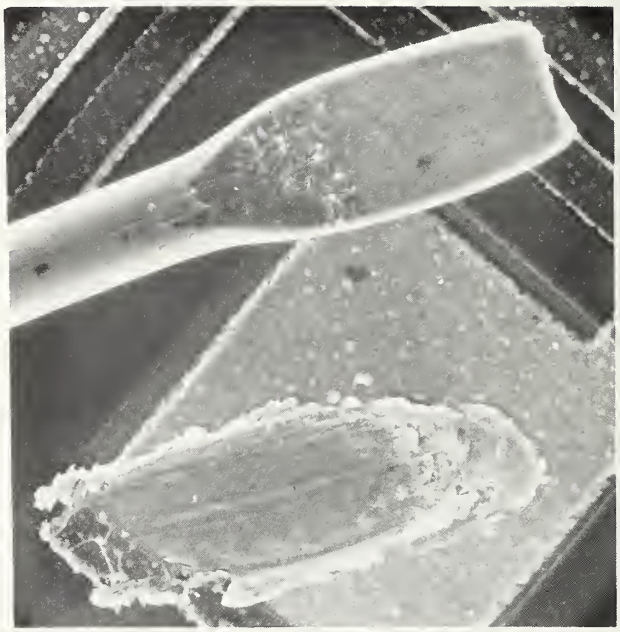

Figure 8. SEM photograph of a weak bond resulting from poor process control. A 25-μm diameter ultrasonic wire bond failure resulting from a layer of glassivation or other contamination on the surface of the bonding pad. The visually perfect bond is shown in the upper part of the figure. The bond lifted at ∿0.2 gf.

This test is used rather extensively in large hybrids and in integrated circuits for space and other applications requiring very high reliability. The NDPT has been reported to cost about half the price of the original wire bonding [7]. Although there is considerable evidence that the test is indeed nondestructive (it has been used on $> 10^7$ wire bonds), it is nevertheless controversial. Some organizations require it on a 100% basis and others absolutely prohibit its use. This test can be both used and prohibited on different contracts for the same electronic system.

2.3.2 Internal Visual Inspection

The purpose of this test is to check the internal construction, and workmanship of microcircuits for compliance with the requirements of the applicable specifications. This test will normally be used prior to capping or encapsulation on a 100% inspection basis to detect and eliminate devices with visually detectable internal defects that could lead to device failure in normal application. It may also be employed on a sampling basis prior to capping to determine the effectiveness of the manufacturer's quality control and handling procedures for microelectronic devices.

Most visual inspection criteria are accompanied by photographs or sketches so that the inspector has a basis for comparison. An example of one of these from MIL-STD-883B [1], Method 2010.3 is shown in Figure 9. Items generally covered by such inspection include placement of wire bonds with respect to the pad, lead dress, device metallization scratches, contamination, obvious passivation and diffusion faults, and die attach faults. Sometimes a scanning electron microscope (SEM) examination of devices on a sampling basis is specified to look for defects such as metallization coverage of oxide steps and diffusion window defects. This is done at the wafer level.

Visual inspection is a relatively expensive test in which much is left to the judgment of the inspector. At best, it is 80% effective in detecting faults and, at times, good product is rejected. If the same device is recycled through the same or a different inspector, different defects are frequently discovered and original ones may pass unobserved. The test is of limited usefulness for large scale integrated circuit chip integrity because of the high magnification and time required. Nevertheless, visual inspection is considered useful and important for removing gross chip and assembly induced defects.

2.3.3 Temperature Cycling

After the package is sealed additional nondestructive mechanical integrity tests are often performed. Some of these follow: The purpose of this test is to determine the mechanical resistance of a part to exposure to various thermal environments that may be encountered during system life. Internal mechanical stresses result from the different thermal expansion coefficients of different parts of the device. This test is the only effective means of revealing very weak aluminum wire

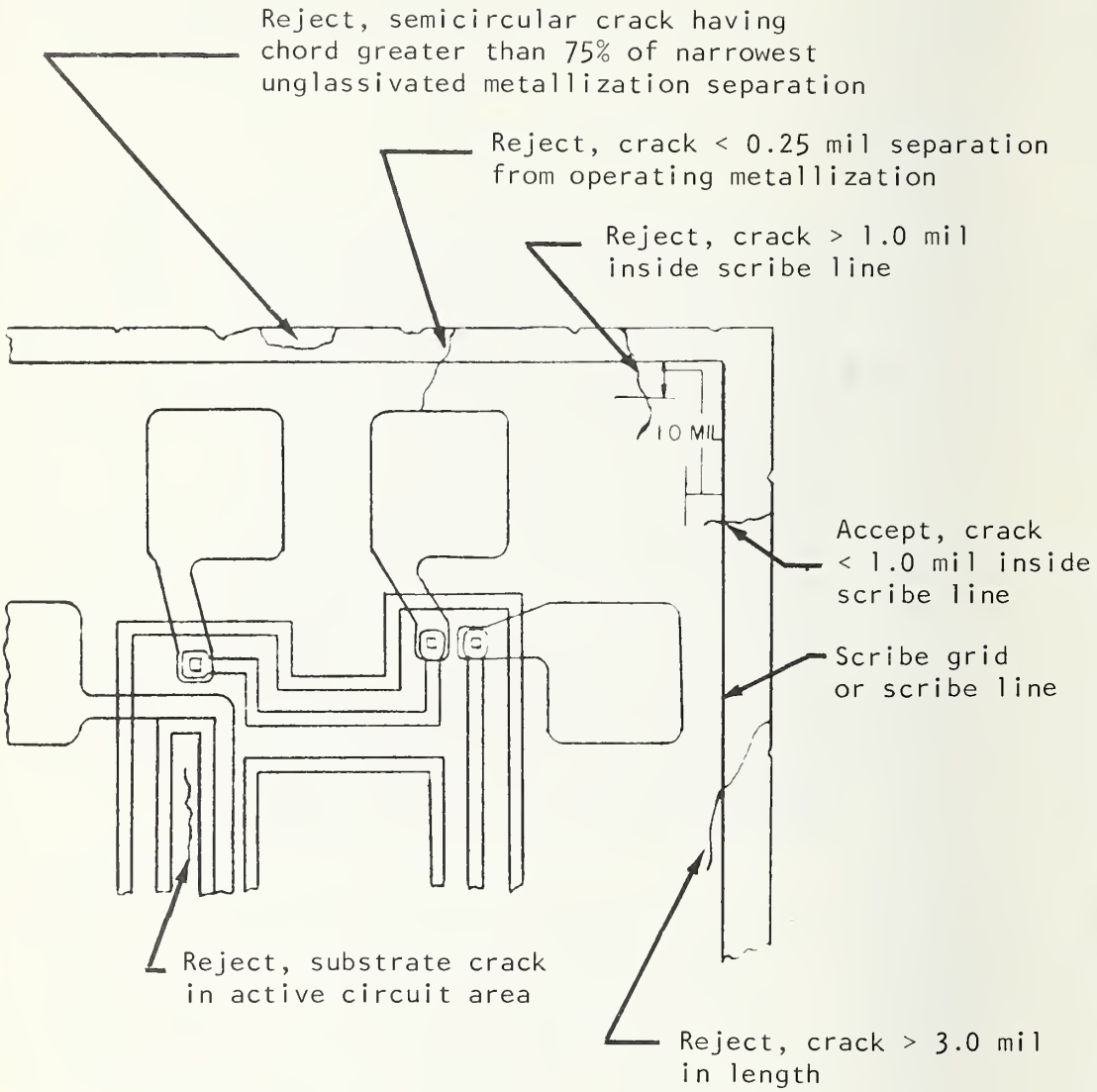

Figure 9. Figure 2010-25 from MIL-STD-883 [1] which is an example of visual inspection criteria for an integrated circuit. Interpretation can be subjective.

bonds after the package is sealed. The test is also effective in revealing poorly welded or soldered caps or damaged glass or ceramic to metal lead throughs.

The apparatus usually consists of two chambers, one cooled and one heated. Many devices are placed in a holder which is rotated or otherwise moved from one chamber to another. Heat transfer takes place by forced air. Typically, the device is tested for 10 to 20 cycles of from -55° to 125°C with 5 minutes equilibrium time at each temperature; but these test conditions may vary depending on anticipated device usage. A hundred or more cycles is usually considered destructive. Temperature cycling is considered an effective mechanical test and is inexpensive to perform. It is usually followed by an electrical test to reveal failures arising during cycling. Temperature shock is a variation of this test. The intent is similar to that of temperature cycling, but shock is a more severe test. The temperature shock test consists of liquid-to-liquid transfer. Although a typical temperature range would be -55° to 125°C, the most severe specified condition in MIL-STD-883 is -195° to 200°C, where the low temperature liquid is liquid nitrogen and the high temperature liquid is a fluorocarbon. The transfer time from one liquid to the other is less than 10 seconds. The test is usually carried out for 15 cycles, where one cycle includes one high and one low temperature immersion. Temperature shock is useful on a sample basis to determine the integrity of package glass to metal seals.

Most operating devices will experience some temperature cycling during system life due to system turn on and off (e.g., automobile engine compartment electronics). However, it is not reasonable to expect a device or system to undergo liquid-to-liquid thermal shock in any anticipated usage. Therefore, if a choice is given, temperature cycling is usually the preferred test.

2.3.4 Package Seal Leak Tests (Hermeticity)

Moisture ingress in electronic packages is the cause of many device failures and, thus, the explanation of leak testing given here will be longer than other nondestructive production line screens. In addition, some of the moisture induced failure mechanisms are worth reviewing since moisture is a major, if not the major, long-term reliability problem for semiconductor devices. The usual point of corrosion attack is the exposed bonding pad aluminum, and subtle metallurgical and contamination induced interactions are common. An example of chlorine-moisture induced corrosion on an IC [8] is shown in Figure 10, and an example of metal migration [9] in Figure 11. One of the less obvious sources of contamination is spittle which may be deposited in micron sized droplets as a production line operator speaks to an associate [8]. The droplets contain contaminants such as sodium, phosphorus, sulphur, and chlorine. The initial water dries quickly, but later after package seal, the deliquescent contaminants may be reactivated by moisture ingress through a leaking package.

Figure 10. Aluminum chloride corrosion product on a glassivated IC chip starting at the gold ball bonds. (After Ebel [8])

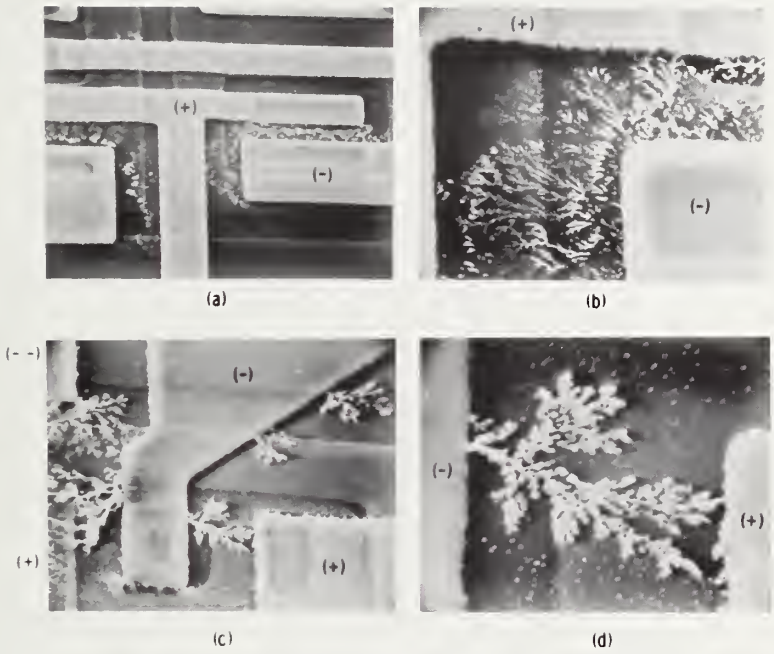

Figure 11. Gold migrative resistive shorts. The (+) symbol is the anode, and the (-) symbol, the cathode. (a) is an SEM view of a portion of a microcircuit showing migrated gold between a T-shaped stripe and two neighboring stripes below the T-bar. (b) is a closeup of the right half portion of the T-shaped stripe. Dendritic or fern-like features between the stripes have been identified to be gold by energy-dispersive analysis of x-rays (EDAX). (c) shows the center stripe as the cathode. Dendrites are shown growing from both sides of the cathode (center stripe) and proceeding toward the neighboring anodes. (d) is a closeup of (c), illustrating the migrated-gold dendritic features typically observed. (After Shumka [9])

The purpose of the various leak tests is to determine the hermeticity of the seal of microelectronic and semiconductor devices with designed internal cavities. There are a number of methods such as bubble, dye, weight gain, halogen leak detection, helium leak detection, and radioisotope leak detection. These have been critically reviewed by Ruthberg [10] and the following treatment is derived from his. There are variations on the methods of performing each test. Because of the small volumes and package constructions, most of the test methods require back pressurization, a process of driving a tracer gas or fluid into the interior by pressurization, and then detection of the tracer on reemission. The bubble, dye, and weight gain methods are appropriate for the gross leak range, which is taken to be $\geq 10^{-6}$ Pa•m^3/s.* The leak detector and radioisotope methods are essentially intended for the fine leak range ($\leq 10^{-6}$ Pa•m^3/s), but can be used for detection into the gross leak range depending on the size of the package internal volume.

Dye penetration techniques are more appropriate to the destructive testing of individual components for diagnostic purposes, where decapping or other physical alteration of the package occurs. Dye techniques are used nondestructively, however for devices with transparent walls. The halogen leak detector method is not frequently used for semiconductor components because of its corrosion potential. Bubble and the helium leak detection are most widely used of all of the leak tests and will be described in some detail.

2.3.4.1 Helium Mass Spectrometer Leak Detector Test

The use of the helium leak detector is well documented. This instrument has the widest leak rate application range for general use. For this procedure, the packages to be tested are pressurized in a simple pressure bomb with helium gas, removed, transferred to the helium leak detector, evacuated, and tested for effusing helium. A numerical indication is obtained from the leak detector which can be related to true leak rate if an appropriate theoretical relationship is available to relate these two quantities. The correlation depends upon the regime of the gas flow into the test object, the pressurization parameters, internal free volume, the delay time between pressurization and readout, and the flow mechanism for helium effusion from the test part. Since enough of the helium must first be driven into the part to give discernible effusion, the pressurization times can be quite long for packages of large internal volume when tested to package leak rates $\lesssim 1 \times 10^{-8}$ Pa•m^3/s. In most standards for helium leak detector use, the package leak rate is determined from an expression based upon the molecular flow regime. The equation is:

---

*Units of flow rate are conventionally atm•cm^3/s or torr•l/s, but in the International System (SI) of metric units the unit of flow rate is the Pa•m^3/s. 1 Pa•m^3/s = 9.86926 atm•cm^3/s and 7.50064 torr•l/s.

$$R = P_b \cdot L \left[\frac{1}{P_0} \left\{ 1 - \exp \left(- \frac{L}{P_0 V} T \right) \right\} \exp \left(- \frac{L}{P_0 V} t \right) \right]$$

where

R = machine reading for helium,
L = package leak rate under conditions of one atmosphere of helium pressure upstream and zero pressure downstream,
P_0 = pressure of one atmosphere,
P_b = bombing pressure,
V = internal free volume,
T = pressurization time, and
t = delay or dwell time between pressurization and readout.

The first exponential term describes the pressure rise of helium within the package due to pressurization, while the second exponential term describes the fall off of pressure due to effusion. Since this expression is based upon the molecular flow regime, it is in principle only applicable to fine leaks; whereas in practice, it is applied to the whole leak range. A double valuedness in leak rate (L) as a function of machine reading (R) and package volume (V) is indicated by the calculation which predicts that a gross leaker may not be distinguishable from a fine leaker without further manipulation of test variables. In practice it is assumed that a minimum and maximum detectable leak rate exists and the range of leak rates between these two limits will be detected for any given bombing pressure P_b (in atmospheres), internal free volume (V) and minimum detectable machine reading (R_{min}).

The failure criteria from MIL-STD-883 is as follows: "devices with an internal cavity volume of 0.01 cc or less shall be rejected if the equivalent standard leak rate (L) exceeds 5×10^{-8} atm cc/secHe. Devices with an internal cavity volume greater than 0.01 cc and equal to or less than 0.4 cc shall be rejected if the equivalent standard leak rate (L) exceeds 1×10^{-7} atm cc/secHe. Devices with an internal cavity volume greater than 0.4 cc shall be rejected if the equivalent standard leak rate (L) exceeds 1×10^{-6} atm cc/secHe."

2.3.4.2 Bubble Emission Tests

There are two classes of bubble tests. One is simply direct immersion of the test object into a hot, clear, inert fluorocarbon liquid of low surface tension. If a leak is present, bubbles will appear as the gas in the device expands on heating. The leak test range is narrow. The second class is superior in test range and detection of leakers. For this, the component is exposed first to vacuum and then back pressurized with a high vapor pressure fluorocarbon liquid so that if a leak is present the fluorocarbon is driven into the component. On immersion in a hot, low surface tension, indicator fluid, the fluorocarbon bubbles out of a leaky device.

Although bubble size and frequency have been related to leak rate under ideal conditions, the interpretation of bubble tests are subjective in practice. They are tedious, results are very dependent upon the geometry of the package, and a gross leak comprised of several fine leaks can be missed. The use of liquids requires that this test be performed after fine leak tests have been completed to avoid the plugging of leaks; it also provides the possibility of residual contamination in the accepted components having undetected leaks.

It has been observed that the tiny bubbles released during the test emit acoustical noise that may be detected in the hundred kilohertz range. Thus it is possible that an acoustic emission type test (see sec. 3) may be developed to eliminate the subjective nature of this test and possibly automate it.

2.3.5 Burn-In Test

The burn-in test is not considered to be a mechanical integrity test (although it may reveal such problems), but it is included in the present discussion because of its importance in assuring device reliability. The burn-in test is performed for the purpose of screening or eliminating marginal devices, those with inherent defects or defects resulting from manufacturing aberrations which cause time and stress dependent failures. These are generally referred to as freaks. In the absence of burn-in, these defective devices would be expected to result in "infant mortality" or early lifetime failures under use conditions. Therefore, it is the intent of this screen to stress microcircuits above maximum rated operating conditions in order to reveal time and stress dependent failure modes in a practical length of time. The procedure involves placing the device in an oven at a fixed temperature for a specified number of hours (e.g., 125^{o}C for 168 hrs) with an applied bias, forward or reverse, depending on the stated test conditions. The regression equations are based on a simple Arrhenius equation derived for the burn-in time (t) where,

$$t = A \exp\left(\frac{E_A}{kT}\right)$$

where A is a constant, E_A is the apparent activation energy in eV (in MIL-STD-883B it is 0.44 eV) chosen for freak population removal, T is the absolute junction temperature, and k is Boltzmann's constant. Figure 12 gives the burn-in regression curve from MIL-STD-883B [1]. This curve is applied to the overwhelming number of devices that are burn-in tested. However the temperature selected must not be high enough to create failure modes not related to freak removal. One such failure mode, known as purple plague (Au-Al intermetallic compound formation [11]), may occur when gold wire bonds are made to aluminum bonding pads. If burn-in is carried out for one hour at 400^{o}C, the interconnects will fail due to this new failure mode.

Various activation energies have been reported for freak populations, 0.25 to 0.7 eV, and main populations, 0.5 to 1.7 eV. These latter vary according to the technology (bipolar $\approx$ 1.1 eV, C-MOS $\approx$ 1.3 eV, beam-lead silicon-nitride sealed-junction $\approx$ 1.7 eV). However, the variations between manufacturers or even wafer lots are often larger than this indicated range of values [12,13,14,15,16].

The freak population produces "infant mortality" and represents devices with relatively gross manufacturing defects. Many different defects may be involved such as cracked chips, nearly open interconnections, oxide pinholes and other oxide defects, mask alignment-induced coverage (oxide or metal) defects, gross contamination and failures that occur earlier than expected from main population failure mechanisms. Main population life may be limited by some of the above causes. It is more often related to ionic drift in oxides, but it may include such process related mechanisms as gold penetration through a barrier metal (for a complex metallization system). Figure 13 vividly demonstrates the different temperature-time dependence of freak and main populations [15]. For this case both the freak population activation energy (0.8 eV) and the main population activation energy (2.0 eV) are quite high, indicative of what is expected from the beam lead type metallization-passivation system.

It has been pointed out by Stitch *et al.* [16] that, in addition to temperature, bias voltage is an important parameter in accelerating failures. In this case the Eyring [16] modification of the Arrhenius time equation is most applicable. It is:

$$t = \frac{G}{T} \exp\left(\frac{E_A}{kT} - V\left[C + \frac{D}{kT}\right]\right)$$

where G, C, and D are positive constants, and V is the bias voltage. This equation indicates that for a fixed temperature as the voltage increases the median life decreases. In one case on increasing the applied voltage from 5 to 15 V, the main population failure mode activation energy decreased by approximately 0.1 eV (apparent) [16]. The problem of directly applying this model results from the fact that in a complex integrated circuit it may be impossible to have the same voltage across each junction, thus one can only speak in terms of voltage applied to the overall device. Interpretation is further complicated by some tests that are carried out at temperatures $> 200^{\circ}C$.

The burn-in test is generally considered to be the only test that can reduce electrical "infant mortality" in electronic systems that incorporate many devices. It is relatively inexpensive to perform and is required on essentially all hermetic military microelectronic devices. The use of this test on nonhermetic (plastic encapsulated) devices can be undertaken only after consideration of such additional factors as the plastic glass-transition temperature and decomposition temperature. Most plastic devices are burned-in at lower temperatures

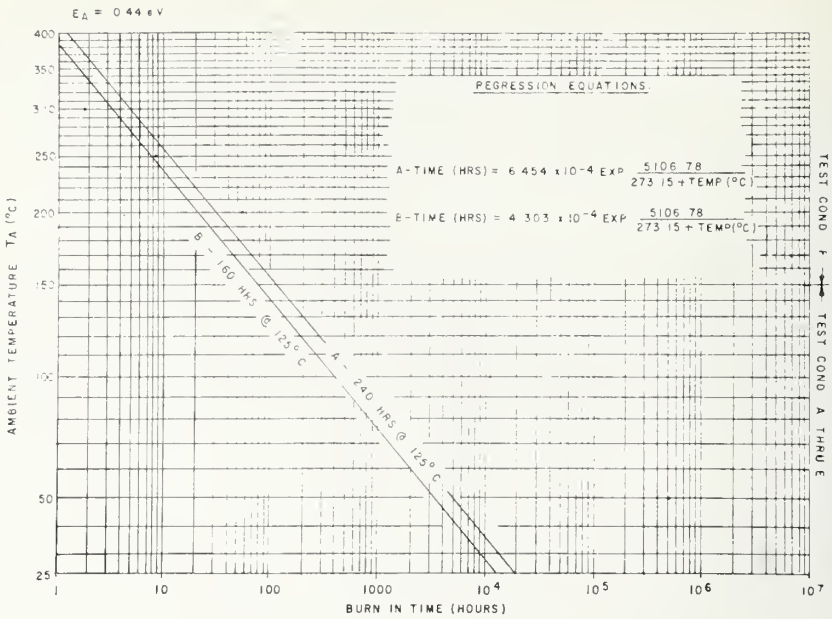

Figure 12. Burn-in regression curve from MIL-STD-883B [1], Figure 1015-1.

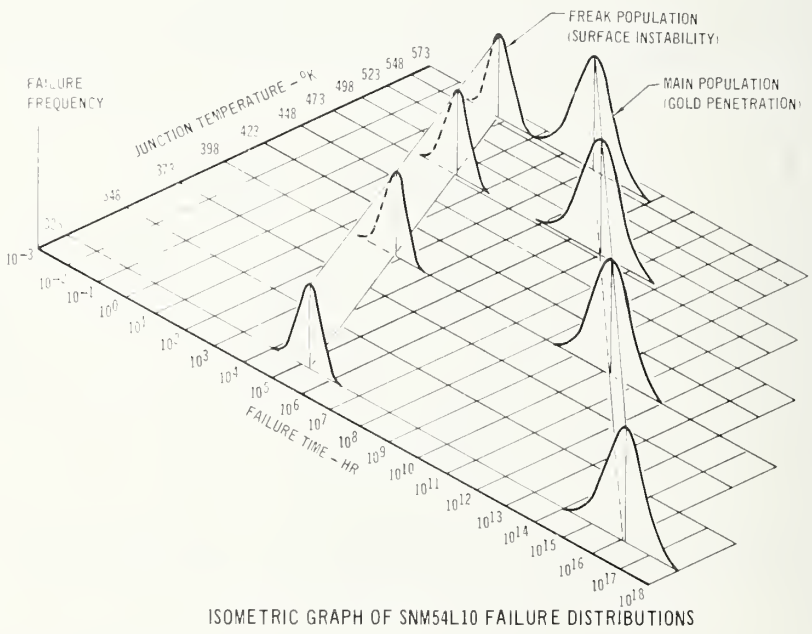

Figure 13. Isometric graph of accelerated test failure distribution for a device with Au-Ti-W metallization showing freak and main population distributions. (After Johnson [15])

than hermetic devices. A comprehensive review of accelerated testing has been given recently by Reynolds [17].

2.3.6 Particle Impact Noise Detection (PIND) Test

The purpose of this test is to detect loose particles inside a device package. To perform this test, the device is attached to a piezoelectric transducer with an ultrasonic couplant material. The transducer is attached to a shaker which vibrates the device and transducer, typically at 60 Hz, at accelerations in the 10 to 20 G level. Various specifications may require different frequencies for different package sizes in order to allow for the variation in time of flight of loose particles with different characteristics. The transducer and ultrasonic amplifier are usually peak tuned to 140 kHz. Most small particles of 25-μm diameter or more will produce ample acoustic signals at that frequency upon impacting with the walls of the device package. Unfortunately, the hissing of compressed air escaping, clapping of the hands and many other common noises may also excite the transducer leading to rejection of good, particle-free devices. Also, some particles do not break loose from the package so that they can be detected during the test. After the device is installed, these undetected particles can cause a failure. Figure 14a shows a wire bond with low lead dress and an arrow points to die attach eutectic particles which could break loose and possibly be detected by a PIND test. Figure 14b shows a loose eutectic particle short between the wire bond and the chip.

The detection systems usually consist of an oscilloscope and headphones or a speaker which are connected to the apparatus through a heterodyne system to reduce the frequency to the audible range. Figure 15 is a sketch of a typical equipment setup for this test.

Before and/or during the test, the device is tapped by a "15 cm solid copper rod 2.5 mm in diameter with rounded end or other apparatus capable of imparting shock pulses of 200 to 1500 G to the device under test" (Method 2020 MIL-STD-883B) to loosen particles adhering to the device or package. Both mechanical and electromechanical apparatus, are available to shock the parts, but because of their differences they may contribute to variability in the test results. Also, different package types display different "personalities" by holding captive similar particles under more or less shock than other package types.*

From this brief description, it should be apparent that this test is neither quantitative nor particularly accurate. In fact, it is controversial. David considers it at best 50% effective [18]. The test is costly to perform and made even more costly because of the ambiguous results. It does not distinguish between metal particles which can cause shorts, and insulator particles that are usually benign. Small particles of aluminum are frequently undetectable. The limit of detection is typi-

---

*Hilten, J. S., Lederer, P. S., Mayo-Wells, J. F., and Vezzetti, C. F., Loose-Particle Detection in Microelectronic Devices, NBSIR 78-1590 (1979).

a

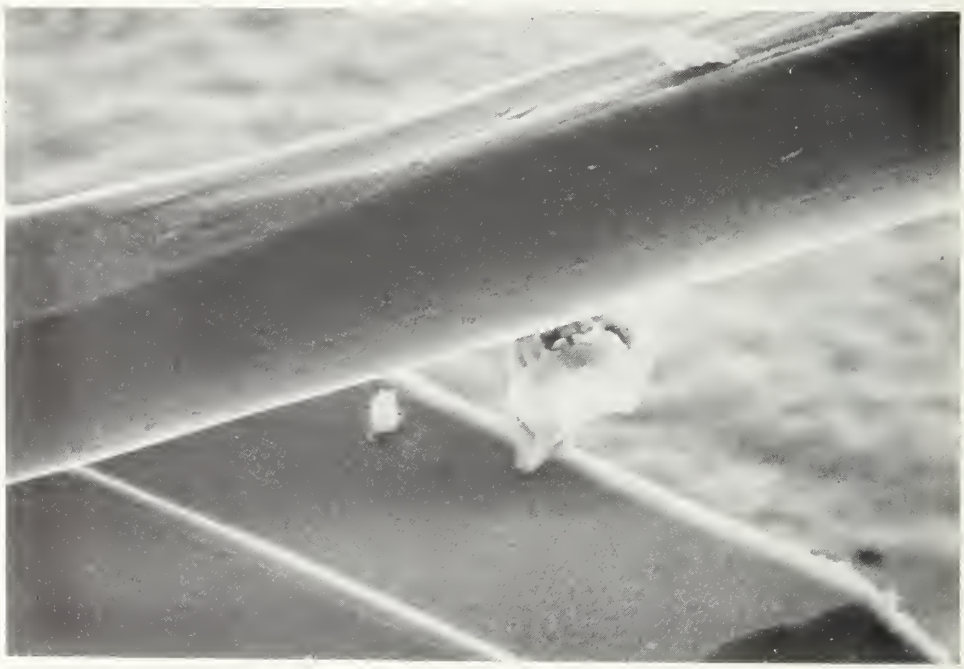

b

Figure 14. (a) An IC having low lead dress and gold-silicon eutectic particles formed during die attach. A typical particle is indicated by arrow. (b), shorting gold/silicon eutectic particle under different lead on same IC. (After Ebel [8])

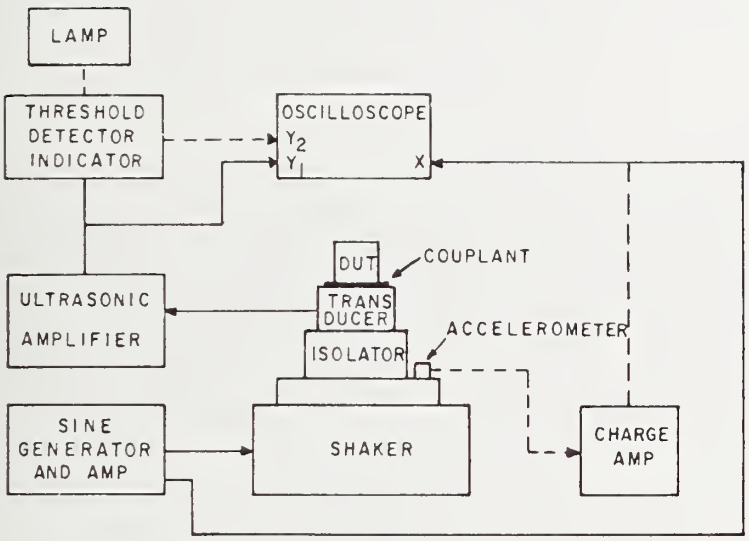

Figure 15. Schematic of typical loose particle detection apparatus from MIL-STD-883B [1], Figure 2020-1.

cally ∿ 0.02 μg, which represents an aluminum particle of approximately 25 μm in diameter.

Even though this test is of limited usefulness, loose metal particles have caused numerous field failures, and a high confidence level test to detect them is still needed. As an alternate solution to the problem, polymer conformal coatings have been used by some organizations to immobilize the particles. This is highly effective, but at times, these coatings can produce their own reliability problems.

2.3.7 The Statistics of Sampling for Special Production Lots

On a production line, all tests, whether destructive or nondestructive, are expensive, and the decision to use one must be a compromise between cost and the reliability confidence level required by the end use of the devices. The costs of applying any individual test are not always apparent to those who must make decisions concerning their use. Implementation of a test is sometimes based on intuition rather than on the physics or statistics involved.

Once implemented, the obvious cost factors of a quality assurance test are the initial expense of test equipment, operator time, and the actual loss of product that results from the test. Some of the less obvious costs are the test throughput time that may cause delays in shipment (such as burn-in or lot-sample life-tests); training of operators; maintenance of equipment; data evaluation costs; record keeping; and the electrical and other costs of running the test equipment (burn-in, lifetests, temperature cycle, etc.). Time lost in making decisions on border line cases (such as in visual inspection of expensive devices), cost of rejecting good product due to incorrect decisions or to such problems as faulty test equipment (e.g., electrical tester with high electrical transients which damage devices or faulty probe adjustments that damage bonding pads).

Because the cost of 100% testing is often prohibitive, various statistical sampling plans have become a normal part of semiconductor device quality assurance. In the past, such plans were generally based on AQL (acceptable quality level), but recently, perhaps because they describe more directly the protection to the consumer for individual lots, LTPD (lot tolerance percent defective) plans are usually specified. MIL-M-38510D [19] contains LTPD tables that are extensively used by the semiconductor industry. This sampling method is valid for special product made in single lots. Parts for space application or other high reliability usage often fall into this category. Also, many hybrids are made and sold in unique lots of 10, 50, or 100 units. The statistics used in controlling the production of parts such as these are not, in general, the same as are appropriate for month after month identical production of a given product, where mean plus standard deviation ($\bar{X}$, S_X) control charts are used to build up confidence. LTPD sampling, as it is practiced in the electronic device industry usually requires segregating production over some period (e.g., 2 hours or a day) from one machine performing a particular assembly or test operation. A number

of devices (determined by the LTPD number) are then randomly selected from the lot and tested. Usually, but not necessarily, if one unit fails (acceptance number, C = 0) the entire lot is rejected or must be 100% tested (if possible) before acceptance. Table 1 presents a portion of the LTPD table from MIL-M-38510D [19]. It should be noted that LTPD is based upon the number of parts tested and not upon the percentage of the lot tested. (If the lot is small, relative to the number to be tested, special calculations are required.)

Figure 16 is a plot of LTPD at defect levels that can be applied to high reliability parts. The values are calculated from a paper by Schilling [20] in which an appendix derives the LTPD equations. It can be seen that a very large percentage of units must be tested to arrive at a low defect level. In fact if the test is destructive, (such as a bond pull test), then it becomes prohibitively expensive and an appropriate nondestructive test is often substituted on a 100% basis (such as a nondestructive bond pull test).

As indicated, LTPD sampling is widely used in industry specifications, and it is almost as widely abused. LTPD plans were specifically derived for protection with regard to single lots, and yet specifications call out the same LTPD values for both single lot and normal, continuous production. Typically in the electronics industry, loose LTPD values of 5 to 10 (% defectives) are specified for all cases. This may result in product of much higher quality than indicated by the specified LTPD when applied to continuous production where a high confidence level, based on $\bar{X}$, S_X charts, is built up over a period of time for the production equipment and personnel. However, the same loose LTPD values are also used indiscriminately for small single lots as well and the user apparently expects lots which pass to have defect levels similar to space parts ($\sim$ 0.1% defectives).

2.3.7 Conclusions of Section 2

Several nondestructive tests (screens) called out in MIL-STD-883B that are applied to establishing the mechanical integrity of electronic devices have been reviewed. Some of these (e.g., the PIND test) result in such a low test confidence level that they should be rarely used, while others (e.g., burn-in) offer considerable assurance against infant mortality or other failures and should be increased in usage. The statistical sampling basis (LTPD) often used in applying these tests was also reviewed.

3.1 PASSIVE ACOUSTIC TECHNIQUES

3.2 Introduction to Acoustic Emission

Acoustic emission (AE) is generally defined as being a transient elastic wave or stress wave generated by the rapid release of energy within a material when that material undergoes fracture or deformation. The classic example of this has been known for years to the metallurgy

TABLE 1. LTPD SAMPLING PLANS[1,2]

Minimum size of sample to be tested to assure, with a 90 percent confidence, that a lot having percent-defective equal to the specified LTPD will not be accepted (single sample).

Max. Percent Defective (LTPD)	50	30	20	15	10	7	5	3	2	1.5	1	0.7	0.5	0.3	0.2	0.15	0.1
Acceptance Number (c) (r = c + 1)	Minimum Sample Sizes																
0	5 (1.03)	8 (0.64)	11 (0.46)	15 (0.34)	22 (0.23)	32 (0.16)	45 (0.11)	76 (0.07)	116 (0.04)	153 (0.03)	231 (0.02)	328 (0.02)	461 (0.01)	767 (0.007)	1152 (0.005)	1534 (0.003)	2303 (0.002)
1	8 (4.4)	13 (2.7)	18 (2.0)	25 (1.4)	38 (0.94)	55 (0.65)	77 (0.46)	129 (0.28)	195 (0.18)	258 (0.14)	390 (0.09)	555 (0.06)	778 (0.045)	1296 (0.027)	1946 (0.018)	2592 (0.013)	3891 (0.009)
2	11 (7.4)	18 (4.5)	25 (3.4)	34 (2.24)	52 (1.6)	75 (1.1)	105 (0.78)	176 (0.47)	266 (0.31)	354 (0.23)	533 (0.15)	759 (0.11)	1065 (0.080)	1773 (0.045)	2662 (0.031)	3547 (0.022)	5323 (0.015)

[1]Sample sizes are based upon the Poisson exponential binomial limit.

[2]The minimum quality (approximate AOL) required to accept (on the average) 19 of 20 lots is shown in parenthesis for information only.

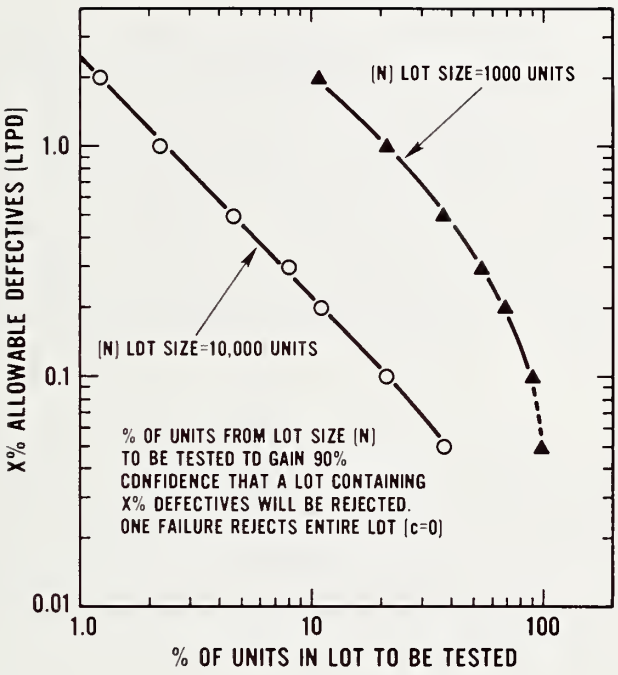

Figure 16. Plot of LTPD *vs.* sample size to be tested at specified defect levels.

industry as "tin cry" where merely bending a piece of tin will result in an audible sound. The first scientific report of sounds being emitted from metals during deformation was given by Joffe [21]. In 1950, Kaiser did the first comprehensive study of the phenomena [22]. His name is associated with the generally irreversible nature of AE, in which little or no acoustic emission occurs until previously applied stress levels are exceeded. Literally, a deformation or crack will only produce more AE if it is enlarged. The emitted stress waves may have frequencies ranging from the audible into the megahertz region, but the maximum energy is usually concentrated in the mechanical resonance modes of the test specimen. Detection of these waves usually takes place with ceramic piezoelectric transducers that are acoustically coupled to the specimen; however, wide band optical [23,24] and capacitive [25] detection methods have recently been used.

Many of the early materials studies were carried out on metals and correlations were made between various metallurgical properties and the AE released after the elastic limits were exceeded in stress-strain type of studies. Dunegan [26], for instance, obtained an excellent fit of a mobile dislocation model for 7075-T6 aluminum, but little correlation was obtained for other metals. The various sources of acoustic emission that have been observed include: crack nucleation and propagation, twinning, grain boundary sliding, multiple dislocation slip, creation of multiple dislocations, solid-solid, solid-liquid, and liquid-solid phase transformations, and the Barkhausen effect (realignment of magnetic domains).

In general, most microelectronic uses of AE, with the exception of certain melt-type welding applications, are more concerned with crack initiation and propagation than with structural dislocations or defects. Crack propagation in brittle materials was first explained by Griffith [27]. He postulated that elliptical cracks exist on the surface of brittle materials such as glass, lowering the tensile strength. Crack propagation occurs when the stress at the ends of the crack exceeds a theoretical value, σ_{th}. The stress (σ_e)* at the ends of such a crack as modified by Orowan [27] is given as:

$$\sigma_e = 2\sigma \left(\frac{c}{\rho}\right)^{1/2}$$

where:

c = the half length of an interior crack or the length of a surface crack and
ρ = the radius of curvature of the ends of the crack ellipse.

For the crack to spread, the stress at the point of the crack must exceed the theoretical breaking stress (σ_b) of the material and

*Units for stress could be grams force/cm^2.

$$\sigma_b = \left[\frac{\gamma E}{4c}\left(\frac{\rho}{a}\right)\right]^{1/2}$$

where:

γ = the specific surface energy and
E = Young's modulus.

It can be seen that as the crack length increases, the stress necessary to keep the crack growing decreases. Thus, once started, complete fracture can occur. The maximum or limiting crack propagation velocity is 0.38 times the velocity of sound in the material.

For brittle cracks in polycrystalline materials, including metals, γ is replaced by γ_p which is the "effective" specific surface energy and c is replaced by d, the average grain diameter. The equation now predicts that the strength of a polycrystalline metal which fails by brittle cleavage should vary as the reciprocal of the square root of the grain size. The energy (E_g) released during microcrack growth, assuming all energy in the grain is released as the crack passes through the grain, is $E_g = \alpha^2\sigma^2$, where α is a constant depending on grain size. Presumably, much of this energy is released in the form of stress waves (AE), although there can be other mechanisms of energy loss. As the crack continues to propagate, stress waves (AE) are propagated in all directions from the crack tip. They include a white spectrum of frequency components up to many megahertz.

Rapid propagation as predicted by the Griffith crack theory, or its various modifications, is assumed to be valid for cracks in silicon chips as well as for glass- and ceramic-to-metal seals as found in semiconductor packages. However, for ductile-metal bonds made under nonoptimized or contaminated welding conditions, this theory is not necessarily correct. As reported in Section 3.4, bonds and various interconnections made under contaminated conditions usually consist of numerous individual microwelds (see Figures 22 and 37) which, in principal, can break individually without propagating a Griffith-type crack. Still, the crack will always propagate along the bond interface without major deformation of the joined pieces. This tends to make crack propagation at least somewhat "Griffith like" rather than what one might expect in an pure ductile fracture. One might calculate breaking stress of such weak "welds"; but the microweld dimensions and number, when made under contaminated conditions, are unknown and this could lead to unrealistic conclusions. Perhaps the closest description of this type of crack propagation has been given for adhesive bond (e.g., epoxy) fracture. Some workers [28] have modified the Griffith equations to include terms for plastic energy dissipation, and others have used a thermodynamic approach. Most are complex and require computer aided computations. Anderson *et al.* [28] have included an excellent review of the theories of adhesive fracture along with the computer techniques used to solve them.

Most aspects of acoustic emission theory are either in a state of controversy or are incompletely developed. Several papers have attempted to develop models that correlate the amount of acoustic emission to the size of a dislocation source, the grain size (for stress wave scattering), and the distance from the AE detector. However, as pointed out by Green [24,29], it is usually necessary to oversimplify the model for purposes of calculation as illustrated in Figure 17a and b. Typically, special point sources and uniform propagation velocities are assumed; but in fact, the sources may have various nonsymmetrical shapes and the emitted wavefront continues to change due to directional variation in wave velocities associated with linear elastic wave propagation in anisotropic solids. Also, the wave amplitude decreases as it travels from the source because of the expanding wavefront and preferential attenuation caused by thermoelastic effects, grain boundary scattering, acoustic diffraction, and scattering from point defects. Some of these attenuation and scattering effects are frequency sensitive. The signal may be further complicated by internal reflections and interferences that depend upon the specimen geometry. Thus, the detected signal amplitude, phase, and frequency may not be characteristic of the source. Therefore, most theory can only be verified on large, simple geometry samples. In addition if the piezoelectric detector has high sensitivity, it usually has a high Q (narrow frequency) response. The amplifiers used for detecting threshold signals usually have a limited band pass to reduce noise, so that all signals are somewhat similar in appearance and ringing is normal. Green [24] has given comparisons between acoustic emission signals from a typical piezoelectric-transducer tuned-amplifier combination and signals from a laser interferometer and optical detector - broad-band amplifier system. The preciseness of the optical detector output is striking as compared to the ringing output of the piezoelectric ceramic transducer system as shown in Figure 17c.

Hsu *et al.* [25] have developed a theory to combine as much information as is known about a simple AE source, its propagation, and detection by a wide band (capacitive) transducer. The theory is based on a Fourier inversion technique. Experiments to verify this theory were carried out on a well characterized system consisting of a 2.5 × 23 × 44 cm aluminum plate with a simulated AE source directly across the smallest dimension from the detector. This system simplified the waveform interpretation and excellent agreement with theory resulted.

It is not even clear how a piezoelectric detector responds to an AE wave front. Harris *et al.* [30] demonstrated that the detector responds to the square root of the energy released during a given deformation process; whereas, Jon *et al.* [31] show that the voltage generated by the transducer is related to the rate of energy released by the source. Thus, with all of the variables and uncertainties, it is extremely difficult to quantitatively relate a microscopic theory of stress wave emission with experimentally measured frequency and waveforms. In addition, it is not clear on a microscopic basis how cracks or other mechanisms actually generate "white" AE.

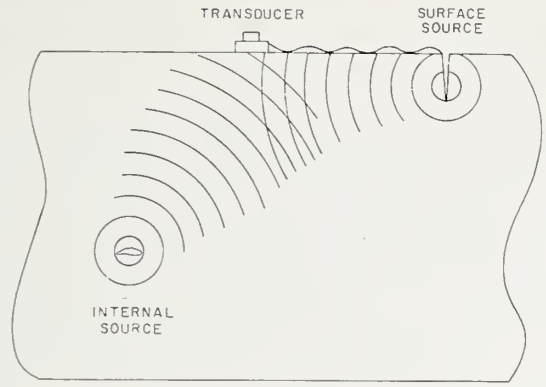

a

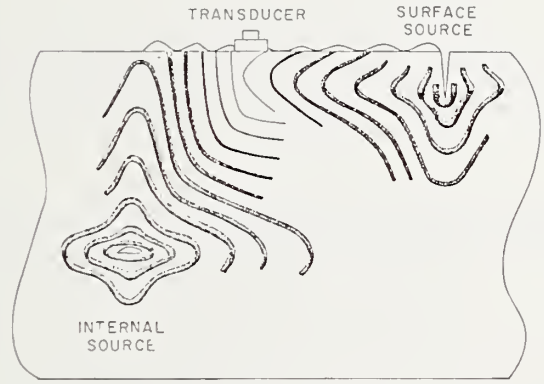

b

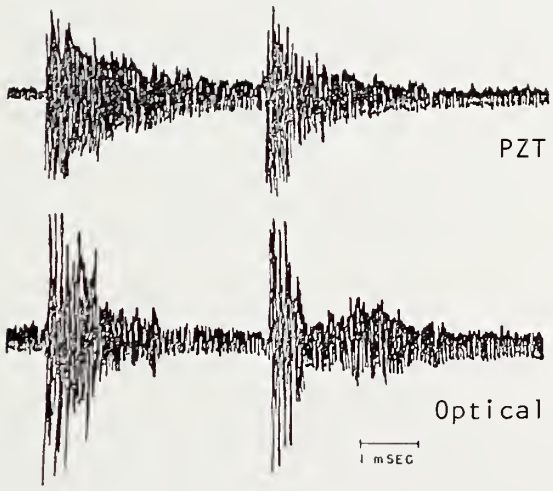

c

Figure 17. (a) Oversimplified model of acoustic emission sources. (b) A more realistic simplified model of acoustic emission sources. (c) Two successive acoustic emission bursts due to stress corrosion cracking; upper trace piezoelectric signal; lower trace optical signal. (After Green and Pond [29])

Many of the concerns of Green [24] and others are not of practical importance to AE detection in samples of dimensions encountered in microelectronics. The various mechanical resonant modes of a specimen may be as high as several megahertz and multiple internal reflections are inevitable. Investigators are usually constrained to attach a transducer, which may be larger than the specimen, in whatever manner is possible (such as using tapered acoustic waveguides) and work with whatever signal is received. Waveform signatures, of frequency and amplitude, are recorded and empirically correlated with appropriate mechanical stress tests (e.g., destructive pull tests) for interpretation. It is obvious that the interpretation of AE signals from typical electronics applications is undeveloped and may never be amenable to clear mathematical solution.

Two books are available that give theory, equipment and applications of acoustic emission to a variety of nonelectronic problems and these should be read for more detail than is given above [32,33]. Also, a recent critical review of the status of the AE field has been given by Lord [34].

3.3 Review of Acoustic Emission Applications to the Real Time Nondestructive Testing of the Mechanical Integrity of Electronic Components

The application of passive acoustic measurement techniques is in its infancy in the electronics industry. Although the potential is great, it is yet to be exploited. Acoustic emission has been used as a tool to study materials and monitor the physical condition of large structures such as nuclear pressure vessels and bridges, but it has only recently been used to evaluate electronic materials and assembly processes. The largest effort is perhaps at the Western Electric Engineering Research Center, Princeton, New Jersey, and a majority of the published papers have come from there. Most of the emphasis has been on real-time, in-process evaluation of some electronic production process and these will be reviewed in this section. These real-time applications will be treated first, and since the present author [35] was responsible for the only study of post-production integrity screening, this subject will be given in greater detail at the end.

The first published use of AE in electronics was by Vahaviolos [36]. He used AE to reveal substrate cracking during the thermocompression bonding of beam lead devices to gold metallization on hybrid ceramic substrates. During this bonding process the substrate is subjected to a temperature of approximately 300^{o}C and high forces greater than 100 kg/cm^{2}. Any ceramic flaw or warping located under the bonding tool may initiate a microcrack, which, if undetected can ultimately lead to failure of the entire device from moisture related causes; or if the crack propagates during later qualification screening or during device life, it may open up a metallization interconnection. A beam leaded substrate of the type and vintage used during that work was shown in Figure 6. The large size and completed cost of the substrate made

it mandatory to stop assembly and reject the unit as soon as any crack was initiated (this problem is even more acute on sophisticated multilayer hybrids).

Since the AE detection work of Vahaviolos required placement of a transducer on the heated bonding stage, he had to make his own high temperature detector mounts and chose piezoelectric sensors according to his special needs. He used a modified lead zirconate titanate transducer which could detect both longitudinal and shear waves and had a curie temperature of 360°C. He also used a lead metaniobate transducer which only detected longitudinal waves but has a curie temperature of > 600°C so that it can be used in many thermal tests.

As in most real-time AE detection systems, the many extraneous production noises that are present must be discriminated against. These may have the same frequency and amplitude characteristics as the AE. For example, during beam lead bonding there is first the impact force of the hot bonding tool against the beams and substrate which generates noise similar to AE. As the beams and the substrate metallization undergo plastic deformation, they also emit AE. If the substrate cracks during this time, a rather sophisticated electronic system is required to distinguish crack generated AE from the extraneous signals. Therefore, most real-time tests are relatively insensitive to cracks 50 to 100 μm in length in brittle materials, whereas a less sophisticated electronics system used to screen completed devices can easily detect brittle cracks 5 to 10 μm long since there are no extraneous signals.

Saifi and Vahaviolos [37] have reported the use of AE for real-time nondestructive evaluation of laser spot welding of small insulated wires to electronic terminal posts. For this, a pulsed YAG laser was used (40 pulses per second, pulse length ∿ 3.5 ms, energy per pulse ∿ 20 J). They determined the conditions required for insulation vaporization as well as for the ideal combination of wire and terminal-post metallurgy (copper wires, monel terminal posts). Production noise was minimized by gating the detection system only during the process period when welding occurred, and after all insulation was vaporized. Although this work is not closely related to microelectronic devices, it could be the beginning of reliable laser welding in smaller structures such as electronic device packages.

Carlos and Jon [38] reported the detection of cracking in high reliability, high voltage ceramic capacitors that were intended for submarine cable use. In this paper, AE is used to detect cracks created in the ceramic casings due to the thermal shock of soldering. Cracks so generated could not be observed in a visual inspection because the susceptible area was covered with solder; however, such cracks could later cause reliability problems. The electronic system was designed to operate continuously and to process each burst of AE from the sensor, using pattern recognition, to determine whether any particular burst resulted from cracking the ceramic or was from such extraneous noise sources as the soldering iron scraping against the ceramic. The system could detect brittle cracks in the order of 25 μm but most actual cracks

were nearer 1 mm in length. This AE system was described as the only possible real-time method of 100% nondestructive checking for cracks in such capacitors.

Jon *et al.* [31,39] have described the use of AE for the nondestructive evaluation of the quality of several types of resistance welds. In one case on tantalum capacitor leads, the material combination in the vicinity of the weld was unique (Ta, Ta_2O_5, Cu, solder, and steel) and it presented considerable AE interpretational problems. For materials of complicated geometry and metallurgical composition, it is not easy to identify any individual intrinsic processes from the total AE generated during the welding process. This identification difficulty is due to the frequent overlap of the generated AE due to different causes. For example, one element of the composition such as copper could begin melting while the already-liquid solder could be going through expulsion from the compressed joint at the same time. Signals generated in such a manner are usually very difficult to distinguish electronically. In such a case, the best way to solve the problem is to monitor the generated AE during a time period where only clearly understood events are occurring. From a metallurgical point of view, the cooling period is easy to identify experimentally. During this period, weld nuggets start to solidify and generate AE signals because of both the plastic deformation and the build-up of the residual stresses. Both of these processes can be used to indicate the weld strength because large nugget volume, a good physical indicator of weld strength, will give rise to more plastic deformation as well as a higher residual stress build-up. The result is to generate more AE signals during this time frame. In order to avoid extraneous AE signals that bore no relationship to weld quality the authors gated their AE detection system to be responsive only from 10 to 40 ms after the peak of the weld current, during the nugget solidification. This period produced AE signals that were directly correlated with weld quality.

Another evaluation of spot welding quality by the AE monitoring of 500-μm diameter nickel wire welded in electronic components was carried out by Knollman and Weaver [40]. The all nickel system was simpler and the wires larger than that described by Carlos and Jon [38]. In this case, a commercial AE weld quality control system was found to be adequate. The authors found that weak welds could be detected at a confidence level of better than 97%.

In 1976, Ikoma *et al.* [41] used acoustic emission to study dislocations in semiconductor materials. Many failures or shortened useful life in GaAs light emitting devices have been shown to result from dislocations propagating into active regions of the device. Also, it had been shown by Kotani *et al.* [42] that improperly controlled thermocompression bonding can create defects in GaAs devices and reduce their reliability. Previously Sedgwick [43] had shown that AE was emitted from dislocation loops in KCl and LiF. Thus, Ikoma designed experiments to explore the possibility of observing similar AE in GaAs by intentionally creating defects. His experimental procedure was as follows. A

quartz rod with a smooth 1-mm hemispherical radius on its end and an AE transducer on the other was used as a pressure probe. The polished GaAs sample was placed on a heat stage. A load of 100 gf was applied in all cases to force the probe against the GaAs sample and the substrate was heated to various temperatures from 25° to 420°C. A study of the dislocation patterns of samples was carried out on the area under the probe by varying the temperature. At each temperature, the sample was etched and the dislocation density and pattern determined. No dislocations were observed to occur below 150°C. At temperatures between 300° and 400°C clear "rosette" patterns were observed with "arms" stretching radially along the $\langle 1\bar{1}0\rangle$, $\langle 01\bar{1}\rangle$ and $\langle \bar{1}01\rangle$ directions on a $\langle \bar{1}\bar{1}\bar{1}\rangle$ surface. AE was only observed at and above 300°C. The AE signal increased linearly with temperature from 300° to 400°C and then decreased above 400°C. The reason for the decrease was not understood, since dislocations were still generated. Since the AE-active temperatures and pressures were the same as those used in thermocompression bonding, it would be logical to apply the results of this investigation to controlling the thermocompression bonding process. Without giving any details, the authors stated, "This technique is now being applied to the detection of dark-line-defects in GaAs-laser diodes and to the real-time inspection of a thermocompression bonding process of GaAs device fabrications."

Very recently, Ikoma *et al.* [44] presented evidence that AE is emitted from GaP light emitting diodes during electrical over stressing. The devices were operated at currents up to three times their rated values. The measurement apparatus consisted of a 4.7-mHz transducer and high gain (69-db), low noise, tuned amplifier. The typical AE signals were very small (∿ 100 nV at the transducer). The authors correlated increased AE with decreased light output. Diodes that showed no decrease in light output produced no AE. After the tests, the devices were etched and those that had produced the most AE displayed the greatest dislocation density. There were large unpredictable variations in degradation from diode to diode. At present, there is no obvious application of the AE correlation with decreased LED performance since the decrease in light output can be more easily measured. However, the authors have clearly shown that electrical and thermal stresses which produce crystal dislocations in semiconductor materials can be revealed by AE. Applications of these techniques for screening out failure prone devices may be possible in the future.

3.4 Acoustic Emission as a Post-Production Screen for Bond Integrity in Microelectronics

3.4.1 Introduction

The previous section reviewed acoustic emission tests that could observe a weak weld or a cracked substrate during the actual production process (real-time). From the standpoint of production economics, this is the ideal time to discover a defect so that no additional production effort and money is lost in further assembly. However, there are numerous cases where such real-time detection is not practical, but instead

a screen applied at a later time is necessary to remove production defects, as with tests in Section 1.1. For instance, in cases of simultaneous multiple bonding such as the 40 lead tape bonding of integrated circuits, it is not possible to assure that all leads are well bonded in real-time. Some stress tests must be applied later. Likewise, when multiple devices are simultaneously soldered, such as in wave soldering, acoustic emission signals are not interpretable. Epoxy bonded components yield little or no acoustic emission during curing, and thus, cannot be tested in real-time. Also, tests are often required as screens for incoming inspection for individual parts such as packages. Thus, the ability to test the component at a later time may be the only way to assure bond or package integrity. The next section describes acoustic emission tests on completed units and will start with tests developed to assure beam lead bond integrity; then the techniques will be applied to tape bonded devices and hybrid components [35].

Beam lead and other gold-gold thermocompression bonding is generally reliable, once an optimum bonding schedule is achieved; however, as with any bonding system, contamination in the bond interface may inhibit welding [45,46] on one or more beams in an unpredictable manner. In addition, if the hardness of the gold varies for devices from different wafer lots or different manufacturers, a bonding schedule optimized for one lot may produce erratic bond reliability for another. Thickness irregularities in thick-film bonding metallization may also reduce bond adherence for one or more beams on a multibeam device. Thus, it is desirable to have a simple 100% nondestructive test that will detect one or two poorly bonded leads out of a large number of well bonded ones and not require a subsequent visual inspection or electrical test to reveal the results.

AE has been studied in a variety of materials by many workers. However, there is only one known study of such emission from gold, the material used in the beam lead bond system. Schofield [47] reported that "the occurrence and behavior of AE in gold was undoubtedly the most consistent and certainly the most active of any of the face centered cubic metals previously studied." He verified the Kaiser effect [22] for the high frequency emission. However, he found that certain "burst emissions" were reproducible without annealing. Schofield's work was on gold single crystals in two orientations; however, some specimens that had been elongated during a first test were then annealed and developed a relatively coarse grain structure. These polycrystalline samples also emitted AE upon further testing. Thus, for the NBS investigation it was concluded that the gold in beam leads should be capable of AE if poorly welded beams lead devices could be stressed adequately to strain or break some of the microwelds in the few bonded areas.

3.4.2 Methods of Applying a Mechanical Stress to the Beam-Lead System

The problem of mechanically stressing a bonded beam-lead device in a nondestructive manner is a formidable one. The most desirable method is to lift the device upward. This would stress both the beam

anchors (the attachment to the chip) as well as the beam bonds. The most obvious method of doing this would be to slip hooks under the corners of the bonded beam-lead device and pull upward. However, since the bugging height* can be less than 25 μm and may vary from corner to corner, such a grappling hook could crack the thinned silicon at the edge of the chip, causing extraneous AE unless extreme care was exercised by the operator. Another method of pulling the device upward would be to epoxy tiny hook-shaped wires to the top of the chip and pull the device with a wire bond puller. A more convenient version of this technique is to use a hot-melt-glue pull-test, applying a force well below the pull-off level. However, the glue used for this purpose would remain on the chip and that particular organic material is not a desirable additive to a hybrid package. Also, the brittle hot melt glue can develop cracks during pulling and emit extraneous, misleading AE.

One simple alternative to the glue method is to apply a "dab" of a silicone rubber (SR) to the top of the beam lead chip and let it cure overnight at a temperature of about 50°C. Then a sharply pointed hook can easily pierce the rubber parallel to the chip as shown in Figure 18. The hook is then pulled upward; about 40 gf can be applied to a 1 × 1 mm chip before the rubber breaks.+ A tweezer type of device or a flatter shaped hook could be used in place of the present hook if it is desired to apply greater pull-forces. To verify that this method produced no extraneous AE, similar sized "dabs" of SR were bonded directly to the substrate and pulled with the hook. The SR emitted no measurable AE until the force that ruptured the rubber was reached. The silicone rubber used for this purpose was usually the stiff version of the methanol-base resin that some organizations use to protectively coat beam-lead devices. When the device is subsequently encapsulated, the new resin will seal the punctured rubber and fill the cavity under the chip. Therefore, this pull method and its residue can be considered nondestructive to both the device and the substrate. Either a 100% test or a sample quantity of devices could be tested on each substrate as a control. Alternately, a high strength silicone rubber can be applied to the chip and this hook method can then be used as a destructive pull test. Pull forces of up to 100 gf have been applied to 1 × 1 mm chips.

Another method of pulling a chip is to mold a vacuum cup out of SR or another elastomer into the shape of the chip. When vacuum is applied to a device, an upward force of about 0.5 gf per beam can be obtained for a 14 or 16 beam device having an Electronic Industries Association registered chip outline. A third method of forcing the chip

---

*Defined as the vertical distance from the substrate metallization to the bottom of the chip.

+If the chip is not clean, this resin may pull free with about 20 to 30 gf. An adequate cleaning procedure is to immerse the bonded substrate in a fluorocarbon solvent and then air blow off the remainder of the solvent.

upward and the beams outward is to inject the silicone protective coating resin under the chip and allow it to cure. The material has a much higher coefficient of expansion than the gold beams. Preferential heat (such as infrared) applied to the chip will expand the rubber enough to stress very weak bonds. This method works best with high bugging heights which allow more resin under the chip.

An alternative method of stressing the bonds is to push downward on top of the chip. Some of the force will be applied to the bond heels in the shear direction. This is also the simplest method of applying force to the beam lead system. Depending on the angle at which the beams project from the chip, the uniformity of the bugging height around the chip, variation in beam dimensions, and the gold hardness, a 16 lead device will collapse to the substrate, accompanied by large bursts of AE, with the application of about 30 to 60 gf. This collapse force may be less if it is applied off-center or if the bugging height is not uniform. An improved variation on the simple push-down technique is to simultaneously push downward on top of the chip and, with an equivalent force, push horizontally along a diagonal of the chip. The force is applied with a molded SR probe that fits over the chip. The advantage of this method is that part of the horizontal force is applied to the bonds in a peel direction. Care must still be exercised to prevent collapse of the bugging height.

It has been found that roughly three times as much force in a downward direction can be safely used if it is only applied to the beams, leaving the chip free. A simple resolution of forces analysis based on typical bonded beam dimensions indicated that with all beams uniformly stressed downward, $\sim$ 90% of the force is applied at the bond heel in the shear direction and no net torque is applied to the beam anchors (the beam attachment to the chip). However, when the beams along only one side of the chip are stressed at one time, the chip is rigidly held in place by the other beams and then essentially all of the applied force appears as a torque on the anchors. Thus, it is possible to provide an AE test for both beams and anchors by appropriately applying the stress. This assumes that the beams project horizontally outward from the chip for about 50 µm before curving downward and bonding occurs about 100 µm away from the chip. In some bonding situations, the beams leave the chip at about 45 deg in a downward direction, and the bond occurs only 25 to 50 µm outward from the chip. No anchor torque is possible in this case. Thus, in order for this test method to be applicable great care in beam alignment during bonding is essential to obtain uniform bugging height.

To determine the effectiveness of the chip push-down method, a simple technique was developed to determine the downward force necessary to produce threshold deflection of the chip as well as of the bonded beams. A 1-mW He-Ne laser with a focused spot diameter of $\lesssim$ 25 µm was directed under the chip at a low angle between two of the beam leads as shown in the sketch of Figure 19. The force was applied by the apparatus described in Section 3.4.4 that is normally used for such purposes

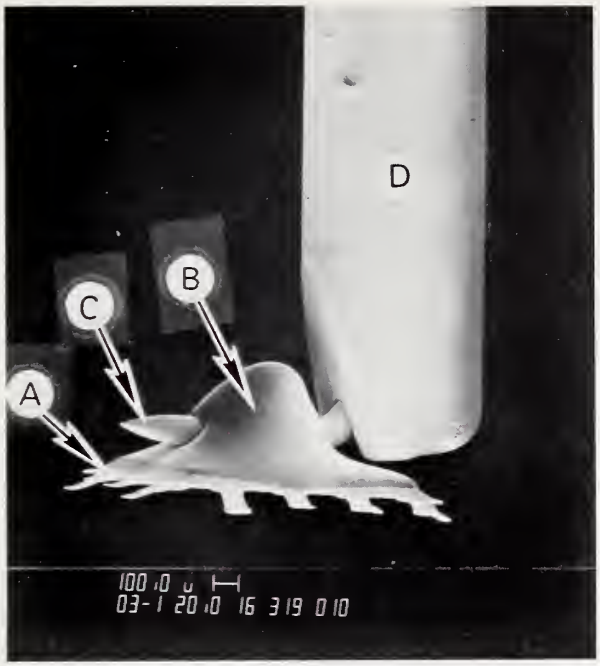

Figure 18. Scanning electron micrograph of a weakly bonded beam lead device (A) with a silicone rubber "dab" (B) on top, that has been pulled up by an electrolytically etched, 150-μm diameter tungsten hook (C). (It is important that the hook be very smooth and have a sharp point so that the rubber is not torn while it is being pierced.) The hook carrier (D) is a section of a No. 22 hypodermic needle in which the hook had been inserted and rigidly epoxied in place.

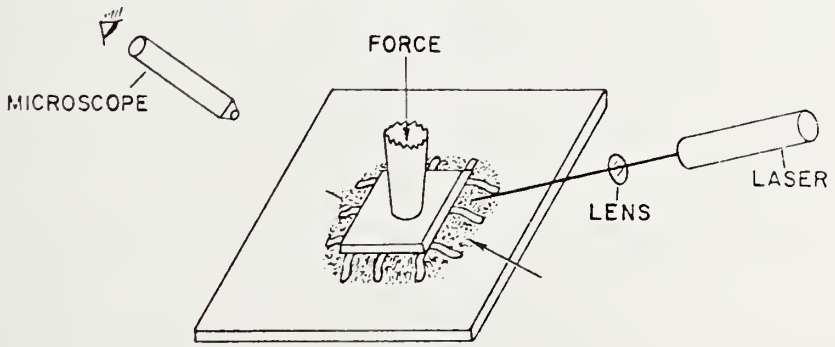

Figure 19. A simple method of measuring the threshold of downward motion of a beam lead chip. The arrow points to the static interference pattern (the dots between the beams). When force is applied, the pattern changes.

in the AE test. The laser light was multiple-reflected back and forth between the substrate and the chip and established a complex static interference pattern that could be seen extending outward from the edges of the chip for 125 to 250 μm. Downward or upward deflection of the chip by only a small fraction of a wavelength produced changes in the interference patterns that could be easily seen through a 40X binocular microscope, even though no direct motion of the chip was discernible. The threshold of observable motion of an individual unbonded beam could also be seen by this method.* Such motion of the chip occurs with an applied force as low as 3 to 5 gf. Essentially unbonded beams require the application of about 10 to 15 gf to the chip before movement is observed, and this requirement varies according to the angle at which the beam lead approaches the substrate.

3.4.3 Preparation of Controlled Bondability Substrates

Various unpredictable bonding conditions can result in one or more of the beam leads not having a strong weld. However, it is difficult to deliberately obtain weak bonded leads. The usual method for obtaining weakly bonded gold-to-gold leads by lowering the bonding temperature is unreliable. The beam leads of such an intentionally weak bonding series that are bonded first may increase in bond strength while other devices are being bonded. Even substrate temperatures as low as 85°C to 150°C for one hour can significantly increase gold-to-gold bond strength on uncontaminated bonding surfaces [45,48], and higher temperatures require even less time for bond improvement. Such strengthening of bonds has been verified in this study. Therefore, low temperature methods of producing weak bonds are not desirable for use in developing new measurement methods.

In order to obtain weak bonds specified in both number and position, an effect that is normally avoided was used. It is well known that chromium-locked-gold metallization must be kept at relatively low temperatures or the chromium will diffuse to the surface, oxidize, and severely decrease the thermal compression bondability [49]. Therefore, tantalum nitride-chromium-gold+ substrates were heated to 310°C for two hours to diffuse the chromium to the surface. A special photomask set was used to pattern the metallization, and a cerric ammonium nitride etch [50] was used to preferentially remove the chromium oxide

---

*Although qualitative in nature, this simple technique may be useful in other types of visual inspection and should be a valuable aid in the observation of the relative thermal expansion of components as well as for studying creep phenomena. In order to be effective, the substrate must be coated with metal. A ceramic substrate under the chip results in a confusing pattern of internal reflections and interference patterns.

+Efforts to use chromium-gold metallizated substrates resulted in rapid etching of the undiffused chromium, thus undercutting the gold. The reason for this is unknown.

in all but specifically designated areas. Figure 20 is a photomicrograph of such a substrate bonded with beam lead devices. For clarity of presentation, the chromium-oxide-covered areas have been darkened (normally they are only slightly darker than the rest of the metallization). The four different patterns can be clearly seen. They include, from left to right, a single poorly bonded beam on a corner location, (D), a single weak beam in the center, (B), two weak beams in the center, and a control pattern for making all well bonded beams.

It should be pointed out that when using the chrome-diffused gold bonding pads, some degree of control over the beam-lead bond-peel-strength (essentially all the bonds so prepared peel) can still be exercised by varying the bonding parameters (force and temperature). In this manner the peel force for an individual beam can be varied from less than 0.5 to approximately 3 gf.

It was established that the chrome oxide method of producing controlled weak bonds still left a few areas that were welded and therefore could produce valid AE signals when the lead was stressed. In addition, it was desirable to determine the minimum AE signals that could be detected with the available equipment. Devices were bonded following various bonding schedules to substrates that had chromium oxide on the surface. The devices were stressed and acoustic emission signals were recorded on digital pulse-capturing equipment. The poorly bonded beams were then peeled back and examined for evidence of torn welded areas representing AE point sources. Figure 21a is an SEM photograph of the chromium-gold coated ceramic substrate with a peeled-up beam in the foreground. Examination of the beam lead bond depression in the substrate revealed tiny broken welded areas around the perimeter where deformation is greatest. The largest of these are indicated by the arrow. The beam is shown in Figure 21b. The tiny white dots near the perimeter are the broken welded areas. The fact that the welded areas lie around the perimeter is in agreement with the deformation theory of thermal compression bonding by Tylecote [51]. A higher magnification view of substrate weld breaks is given in Figure 22. It should be noted that the bonds made under such contaminated conditions consist of a large number of individual microwelds. Each one of these may be broken relatively independently of distant ones, and thus, this type of bond does not necessarily follow the crack propagation velocity as described in 3.2. The arrows in the figure designate broken gold welds of one to two micrometers width. Figure 22b shows part of the beam-lead, clearly revealing pulled-off metal pieces from the substrate. In this case, their size is two to three micrometers in width.

3.4.4 Experimental Apparatus

Most mechanical stressing experiments and AE measurements were made using the apparatus of Figure 23. The force gage (A) can measure either an upward or downward force. The entire gage-probe apparatus can be rocked in front-to-back and side-to-side directions by the knob (B) enabling a downward or upward force to be applied at an angle to a single row of leads at a time. The top AE detector-force probe (C-D)

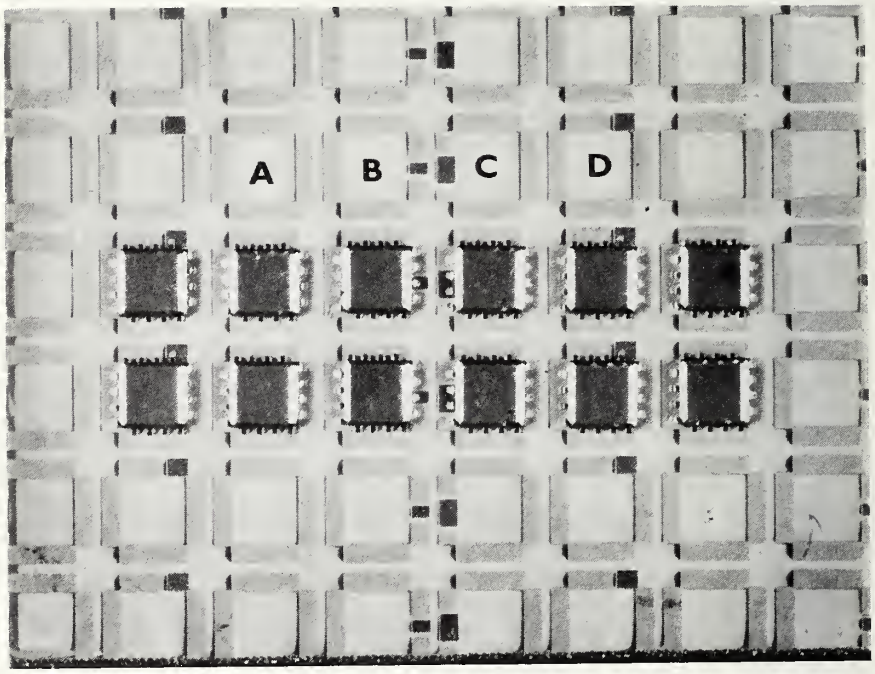

Figure 20. A patterned substrate showing bonded beam lead devices. Chromium-oxide-covered areas for bond strength inhibition are stained black to increase visibility. The vertical row patterns are: (A) bonding controls (all good bonds), (B) pattern containing one weak bond in the center of the span, (C) pattern containing two weak bonds in the center, (D) pattern containing one weak bond on a corner. The chip dimensions are 1 mm on a side.

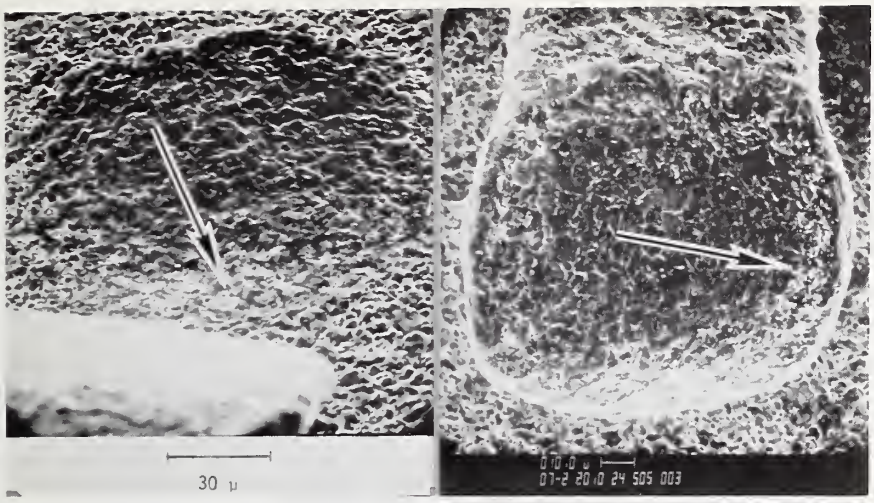

a b

Figure 21. (a) is an SEM photograph of a chromium-diffused, gold-coated ceramic substrate with a peeled-up beam lead in the foreground. An arrow reveals some of the tiny broken substrate welded areas. (b) is an SEM photograph of a peeled-up beam lead revealing the tiny white-appearing dots near the perimeter that were the welded areas.

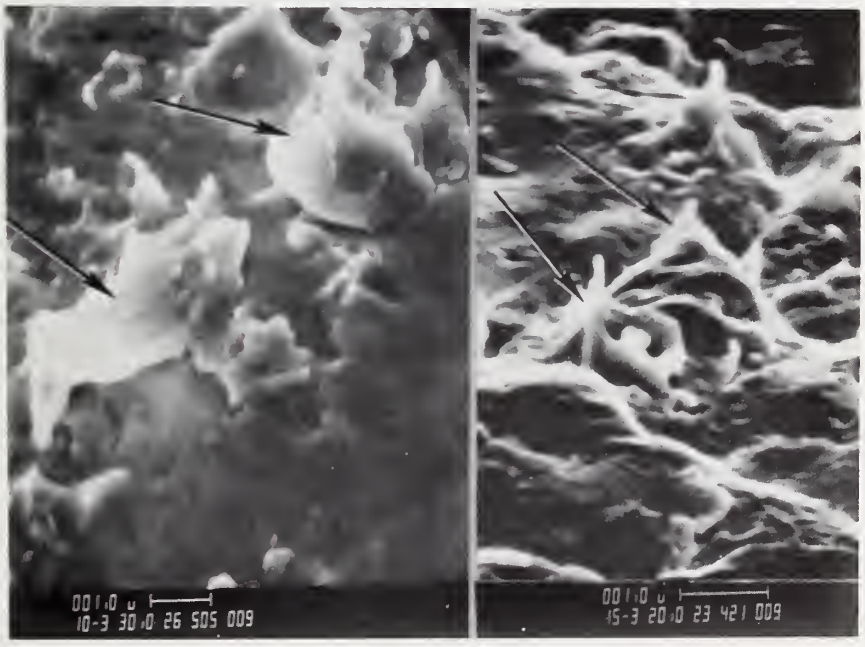

a b

Figure 22. (a) is the SEM photograph showing pieces of the substrate pulled off and sticking to the beam lead. (b) is a high magnification SEM photograph of substrate weld breaks. (These are indicated by the arrows.)

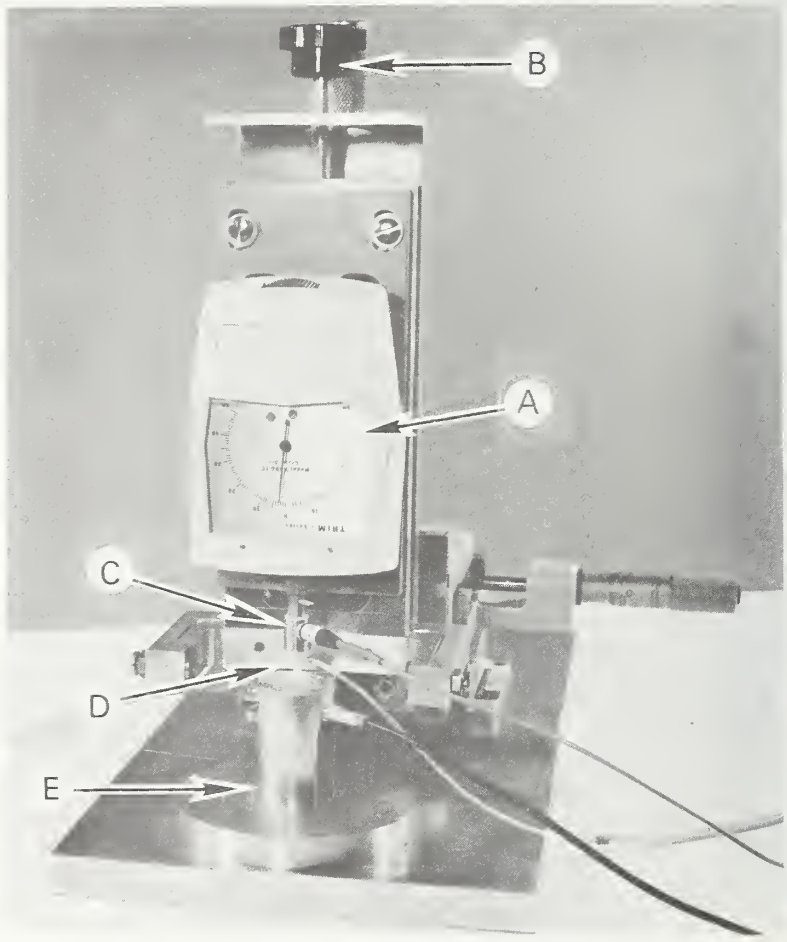

Figure 23. Apparatus used to apply upward or downward force on beam lead devices and to detect any resulting AE. (A) force gage, (B) force angle control, (C) acoustic emission detector, (D) acoustic waveguide and force probe, (E) substrate holder with vacuum hold down and substrate AE detector.

is screwed into the gage, facilitating rapid probe changes. The bonded test substrate is held on a chuck (E) which contains the substrate AE detector.

Close-up photographs of several top detector probes are shown in Figure 24. Figure 24a shows a ceramic probe designed to apply a uniform pressure on beam lead chips. Figure 24b shows a tungsten carbide conical probe with a 75-μm diameter flat on the bottom. This probe is used to stress individual leads. The probe in Figure 24c is made of tungsten carbide and is essentially a beam lead bonding tool with small dimensions so that it only contacts the horizontal projection of the beam near the silicon. The tips of all probes are coated with from 25 to 75 μm of SR both to increase the acoustical coupling to the leads or chips and to avoid metal-to-metal or metal-to-silicon contact since such scraping can result in extraneous AE-type noise.

A substrate detector fixture is shown in Figure 25. In this particular fixture, the test substrate is held against the AE detector by a cylindrical weight. (Other substrate detector fixtures such as the one that was shown in Figure 23 use a vacuum hold down.) The detectors are forced upward against the substrate by a spring. The surface of the substrate detectors are coated with a thin film of very compliant SR to facilitate acoustical mating with the ceramic substrate, in order to avoid the use of various sticky organic coupling materials which must be removed later. A textured SR surface is preferable. This is obtained by pressing ground glass, treated with a mold release agent, against the detector while the resin cures.

Several arrangements of signal preamplifiers, filters, and the transient recorder have been employed. However, the block diagram of the most frequently used system is given in Figure 26. The total gain in each amplifier channel is 80 dB. Each channel has a 24-dB/octave band pass filter, a tunable filter, or both. The special digital trigger circuit [52] requires that a given number of cycles, selectable from 1 to 10, of a separately specified positive and negative amplitude signal occur within a total specified time frame for triggering the dual-channel transient recorder. The overall system is capable of detecting AE signals barely above the average noise level of the preamplifiers and considerably below various system and line transients. Most AE detector output signals produced in the present experiments were in the range of about 10 to 100 μV and were easily captured by the above equipment. Because of the variety of gain adjustments possible (preamplifiers, pulse capturing equipment, and oscilloscope), the vertical scale of most AE oscillograms will not be specified. The only important consideration is the signal-to-noise ratio and this can be easily observed from the traces.

Experiments were run using various AE substrate detectors with the tunable filter. It was found that the maximum AE output was obtained from the thin, 2.5-cm square ceramic substrates at 350 to 400 kHz, and from bonded 16-lead, beam-lead chips at approximately 1 MHz. The actual boundary conditions were unknown and could not be included in equations of the mechanical resonances of the substrate and chip, and thus calcula-

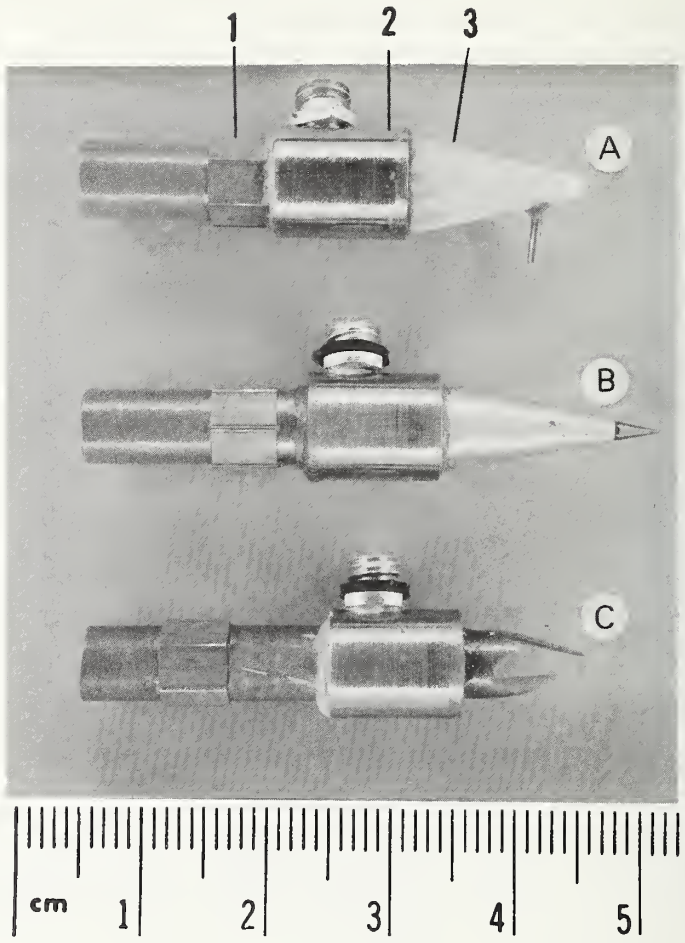

Figure 24. AE probe-detectors. (1) Adaptor for attachment to the force gage, (2) AE lead zirconate titanate type detector, (3) acoustic waveguide and probe. Probe (A) is designed to apply uniform pressure on SR encapsulated beam lead chips. The waveguide portion is ceramic and its tip is coated with SR or polyamide. Probe (B) is designed to probe individual beams. The center tip is of tungsten carbide and has a 75-μm flat portion which is coated with SR. Probe (C) is a modified tungsten carbide beam-lead bonding tool in which the inner walls are about 25 μm larger than the silicon chip on all sides.

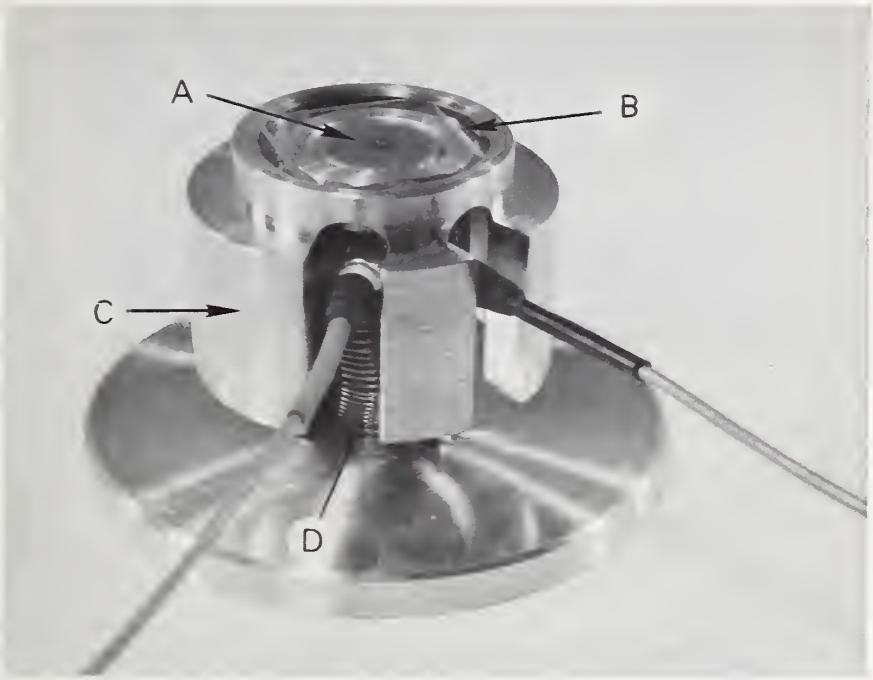

Figure 25. Substrate holder using a weight to force the substrate against the detector. (A) AE detector, (B) simulated substrate (glass), (C) removable brass weight, (D) spring to force the detector against the substrate.

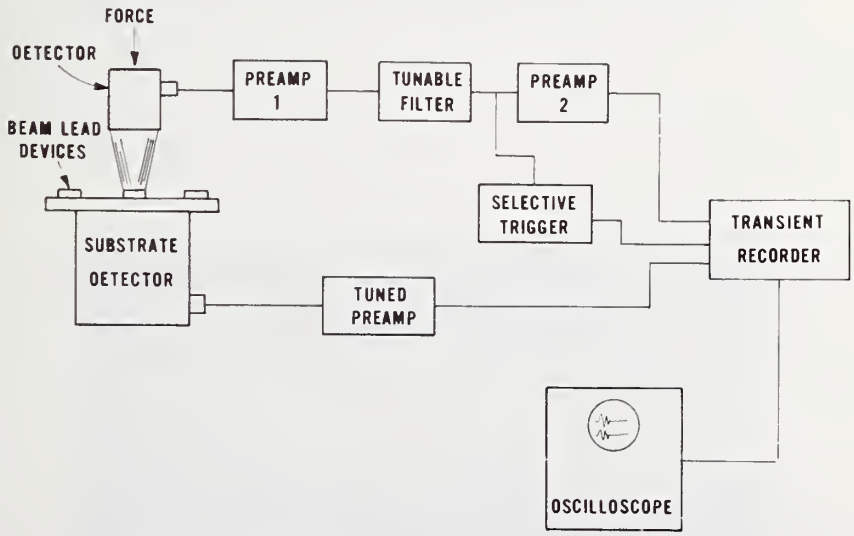

Figure 26. Block diagram of the acoustic emission test apparatus.

tions were off by more than a factor of two. As a result of the measurements, the substrate preamplifiers and detectors were chosen to peak at 375 kHz and the chip probe equipment at 1.1 MHz. The AE experiments described here will all assume such frequency responses unless otherwise stated. The digital trigger has been used in either the substrate or probe circuit; but in most cases, it was used in the probe circuit.

When the probe was in contact with the chip, there was essentially no mutual response from the probe and substrate detectors resulting from random AE sources remote to the beam lead device, regardless of the operating frequencies of each detector. A crack in the substrate would yield a strong signal in the substrate detector, but not in the probe. A ceramic scribe-scratch on the tapered probe, which saturated its detector preamplifier, was only negligibly registered on the substrate detector. However, stress waves generated by a failure within the beam bond-anchor system resulted in a substantial signal in both channels. Therefore, in experiments where both substrate and probe detectors were employed, some AE output was required from each detector in order to define a failure, although their relative amplitude as well as the number of bursts recorded from each detector often varied considerably when the detectors were operated at different frequencies. The purpose of the present study was to develop a specific test method; however, monitoring a single AE source in two or more frequency bands, as in the present experiments, may be a fruitful approach to understanding the nature and mechanism of stress wave emission.

3.4.5 Experimental Results

3.4.5.1 AE Results from Pulling Beam Leaded Devices

The silicone rubber-hook method of pulling beam-leaded devices, as described in Section 3.4.2, was used to obtain quantitative information of various beam failure modes, since the pulling force is equally distributed between all beams. For this work the apparatus of Figure 23 was used. The hook shown in Figure 18 was substituted for the probe detector and all AE was picked up by the substrate detector.

In order to demonstrate the sensitivity of the AE method, all beams except one were cut and the remaining one was pulled to destruction. It broke at the bond heel. Figure 27 gives its AE pattern. Clipped waveform peaks indicate that the substrate detector output was significantly greater than one millivolt peak to peak during the initial part of the break. AE from such breaks generally continues erratically for several times the 200 μs shown in the figure. Most AE signals in this work are much smaller and of shorter duration. For comparison a well bonded device with weak anchors had all but one of its beams cut in a similar manner to the above. Figure 28 gives the AE pattern of the single anchor failure. The peak-to-peak detector output in this case was approximately 0.3 mV.

Pull tests were conducted on several well bonded devices that had weak anchors (peel strength $\sim$ 3-gf/anchor), a series of short bursts

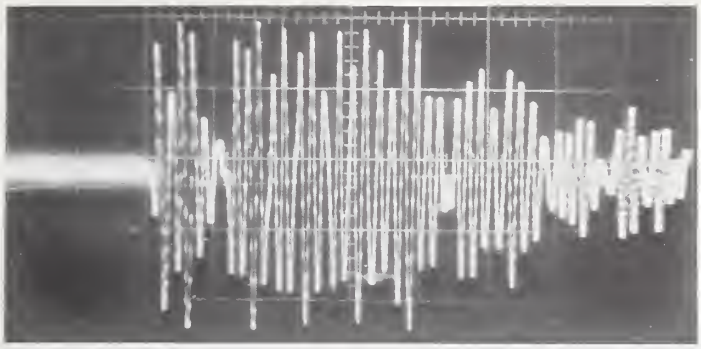

Figure 27. Oscillogram of the AE obtained from pulling off a single well-bonded beam lead with a force of ∿3.5 gf. Horizontal scale is 20 μs/div. The peak-to-peak output of the detector was greater than 1 mV.

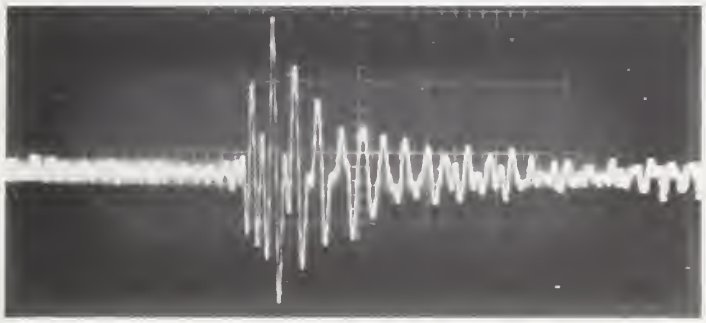

Figure 28. Oscillogram of the AE obtained from a single anchor peeling off under a load of ∿3 gf. All other leads on the device were cut. Horizontal scale is 16 μs/div.

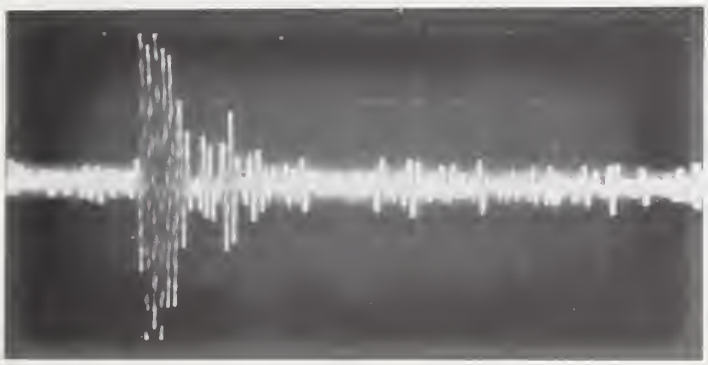

Figure 29. A typical AE burst from a weak anchor. A pull-force of only 1.5 gf/beam was applied. The entire sweep is 200 μs in duration and the main AE burst is about 15 μs long.

was observed starting at ∿ 1.5-gf/beam. Figure 29 gives a typical AE signal from peeling anchors. Similar well-bonded devices with strong anchors produced no AE until a force per beam of approximately 2.5 gf was applied and the bursts in this case were longer and higher in amplitude.

Pull tests were conducted on strongly bonded beam-lead devices to serve as controls for weakly bonded-beam experiments. A number of devices from four different manufacturers were tested. The devices from three of these manufacturers produced no detectable AE until stressed to about 2.5-gf/beam, at which point the beam and the anchor system began to deteriorate. However, devices from the fourth manufacturer were quite different. Large bursts of AE were emitted when the devices were stressed to only 1-gf/beam and these bursts increased with increasing stress. This result was verified on three different device types and on lots purchased 18 months apart. Examination of these devices after they had been stressed to the 1-gf/beam level revealed no obvious problems; however, examination of them after stressing to the 2.5-gf/beam level (the point where well bonded devices from other sources generally emitted their first AE bursts) revealed elongation of the beams, separation of the relatively thick titanium layer, anchor peeling, nitride separation from the beams or silicon, and chips of silicon broken off at the anchor location (see Figure 30). Figure 31 gives a typical AE burst obtained by pulling a similar device to 1.2-gf/beam. Any of the mechanisms of beam system degradation shown in Figure 30 could be responsible for bursts such as that of Figure 31. It should be noted that a normal destructive pull-off or push test would not have revealed any problem since these beams ultimately broke with forces similar to those from other sources.

Poor mechanical integrity could possibly lead to premature electrical problems resulting from thermal cycling if the device is encapsulated in silicone rubber (SR). Dais [53] has calculated the forces on the beam lead system during bonding, and although not explicit in his calculations, it appears that forces high enough to produce beam system degradation may occur during bonding. If so, the devices with poor mechanical integrity could be damaged during the bonding process and predisposed to relatively early field failure. It should be emphasized, however, that there is no experimental proof of this possible result of poor beam-anchor mechanical integrity, since no electrical tests have been performed in this study.

In a large series of SR pull tests on devices bonded to the chrome diffused substrates shown in Figure 20, it was found that a pull force of between 1.0- and 1.5-gf/beam was required to produce AE from one or two weakly bonded beams on an otherwise well-bonded device. A lower force, of between 0.5- and 1.0-gf/beam, was often sufficient to produce AE when all of the beams were poorly bonded (i.e., the device would pull off at a force of 1.0- to 1.5-gf/beam).

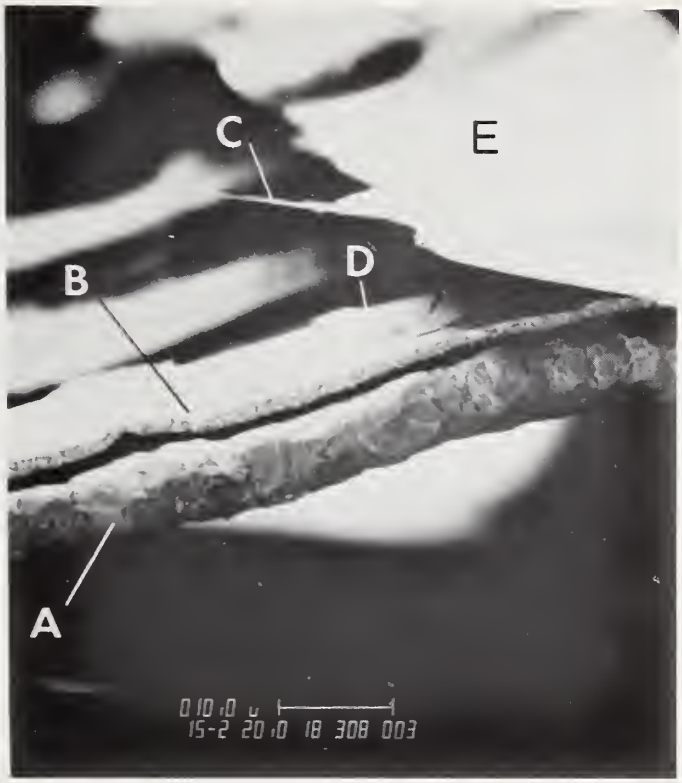

Figure 30. SEM photograph of a beam lead from a device having poor mechanical integrity. The device had been subjected to a pull force of approximately 2.5 gf/beam. (A) gold beam, (B) separated titanium layer, (C) silicon nitride, (D) broken piece of silicon, and (E) silicon chip.

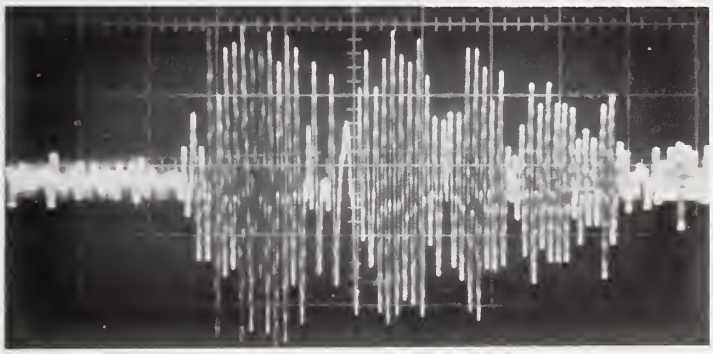

Figure 31. An AE burst from a device having poor mechanical integrity as shown in Figure 29. The pull force to produce this burst was only 1.2 gf/beam. Horizontal scale is 20 μs/div.

3.4.5.2 Tests that Apply Force Only to the Beams

The two silicone rubber tipped probes, designed to avoid contact with the chip, have been used to apply a downward force on the horizontal portion of the beam extending outward from the chip. As previously stated, the simple resolution of forces analysis of a single beam indicates that approximately all of that force is applied as a torque tending to peel the anchor. Thus, probing a single beam or a single row of beams along one side of the chip provides an anchor adherence test. If all beams are probed at the same time, the torque cancels out, and force is applied only to the bond system.

Individual beams were probed with the silicone rubber tipped tungsten carbide probe shown in Figure 24b to establish AE patterns for both anchor and beam failures. Figure 32 gives the twin AE oscilloscope traces resulting from applying a downward force of approximately 2 gf to a beam with a weak anchor. The anchor failed at an applied force of 3.5 gf. A well bonded beam having a strong anchor would typically collapse (curve downward until it touched the substrate) with a downward force of from 6 to 10 gf depending on the beam curvature and the bugging height. The beam-probe AE detector usually produces a larger signal than the substrate detector for anchor failures. When a very weak bond (failing at $\lesssim$ 1-gf/beam pull force) is probed in a similar manner to about 3 or 4 gf, the AE signal intensities are generally reversed, as shown in Figure 33. However, it should be emphasized that, while these are typical AE patterns for their respective failure modes, those same failure modes may at times produce entirely different patterns.

Some experiments were performed using the single probe to try to detect AE from silicon nitride breaks. In general, breaks in the thin ($\sim$ 2000 Å) nitride skirt were not detected under normal circumstances. This was believed to result from higher frequency emission as well as poor stress-wave coupling into the chip and substrate. This was verified by coating the single beam probe with a viscous acoustic mating compound and moving it sideways into an extended nitride skirt. A small AE burst was recorded in the probe detector circuit (1.1 MHz) but not in the substrate detector.

3.4.6 Application of Acoustic Emission to Determine the Integrity of Tape Bonded Devices and Hybrid Components

There are a number of semiconductor device areas in which AE can be used to insure mechanical integrity. One of the most straightforward uses is in testing to assure the bond integrity of automated tape carrier systems. To do this automatically, the mechanical stressing of bonds may be accomplished as the carriers bend during winding on a reel. A rubber coated detector could be pressed against part of the inner bonded lead frame as the frame undergoes some maximum allowable flexing or bending during or before being wound onto the reel.

To show the feasibility of this procedure, some AE tests were performed on different types of automated gang-bonded integrated cir-

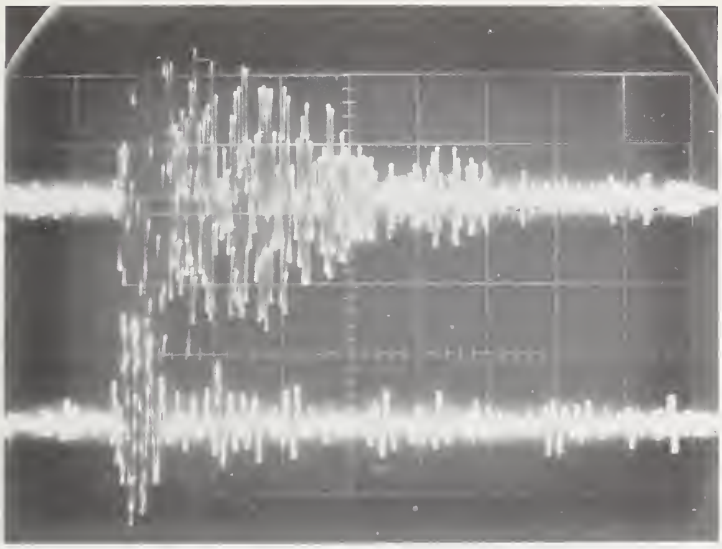

Figure 32. AE output from applying a downward force of ∿3.5 gf to a single well-bonded beam that had a weak anchor. The horizontal scale is 20 μs/div. The upper trace is from the probe of figure 23(B) (peak response is 1.1 MHz). The lower trace is from the substrate detector (peak response is 375 kHz).

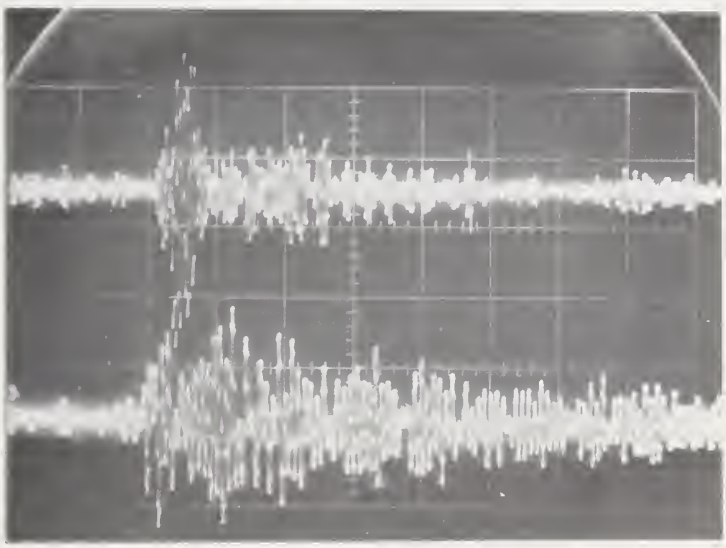

Figure 33. AE output oscillogram resulting from a downward force of ∿4 gf with the probe of Figure 24(b) on a single very weakly bonded beam (∿1 gf pull force). The scales are the same as in Figure 32.

cuits. The first was of solder bump-Kovar inner-lead construction. A slight bending applied 2 gf per lead to the uncut inner-lead frame and produced the lifted lead shown in the upper illustration of Figure 34. The lower illustration of Figure 34 shows the substrate detector response to the AE resulting from that single bond lifting. Examination of this device and others from this lot revealed a tendency for the solder bump and its interfacial plating to separate from the aluminum bonding pad. A second type of gang-bonded device having an aluminum inner-lead construction was tested in a manner similar to that used for the solder bump unit. One of these devices had several weakly bonded leads which emitted bursts larger than that shown in Figure 34 when they separated. Similar tests on several modern tape bonded devices reveal no failures even though the visual appearance of one was quite poor, see Figure 35. Destructive pull tests verified that both of these leads were well bonded. Thus, it appears that an AE test can be used to assure bond integrity on such gang-bonded systems. In addition, it showed that a lead that would have been rejected in a visual inspection was adequately bonded.

Failure was indicated by AE in the above cases when the lead completely lifted up. Low stresses applied to weak bonds on similar device structures often gave preliminary warnings of peel failures that would later occur at higher forces. Figure 36 is the AE burst from a lead that partially lifted up at a stress of 6 gf. Later the lead completely lifted at 14 gf. This is a demonstration that a catastrophical Griffith-type break (see 3.2) is not necessarily valid for typical tape bonded leads used in integrated circuits and that the microwelds are capable of breaking, perhaps in groups; but a peel (crack) may be arrested part way into the bond and not propagate further until a higher stress is applied. An investigation into the fracture mechanism of this weakly bonded system revealed that the copper lead to gold plated bump weld contained numerous individual microwelds similar to those of Figure 22 for the gold-gold system. The only difference was the mode of fracture which was frequently the "cup fracture" type, characteristic of OFHC* copper [54]. Figure 37 shows two such copper cups remaining on a gold plated bump after the lead had lifted at 14 grams.

A different metallurgical tape bonded system was shown to give AE results that were not correlated with the bond integrity. This system consisted of gold bumps on the chip and tin plated copper leads on the tape. During the process of thermocompression bonding the tin melts and may form intermetallic compounds with the gold bump, as is evident in Figure 38. These compounds are relatively brittle, and if the lead is stressed, they can crack at comparatively low forces. Such cracks are shown in Figure 39. The upper lead cracked at 5 gf and was further stressed to 10 gf with no additional AE. The lower lead was stressed at 4 gf and cracked. It was further stressed to 7 gf with no additional AE. Figure 40 is a close-up of the lower lead with the AE burst associated with the small double crack. Upon further stressing, these two

*A pure grade of copper "oxygen free high conductivity."

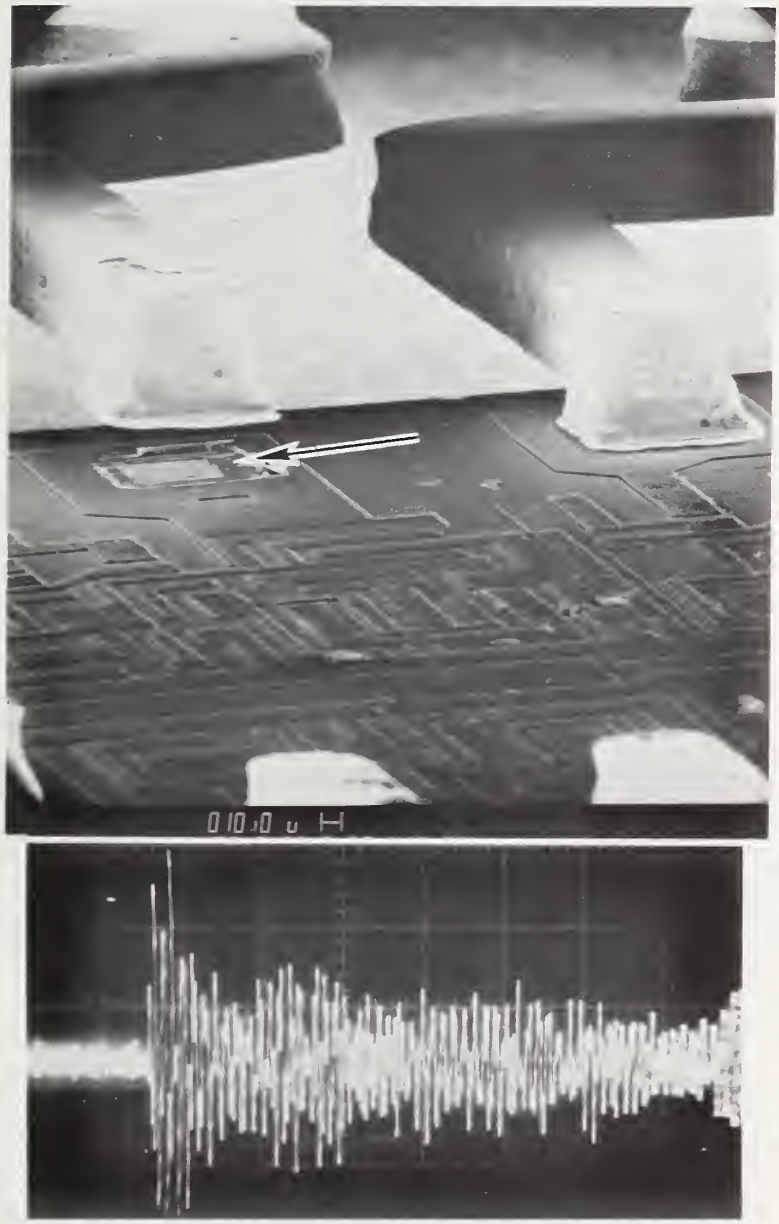

Figure 34. The top illustration is an SEM photograph of a portion of an automated gang-bonded integrated circuit. The bond on the left lifted up during minimal bending of the lead frame. The lower illustration is the AE waveform resulting from the lift up. The signal was picked up by the substrate detector peak tuned to 375 kHz. The horizontal scale is 20 μs/div.

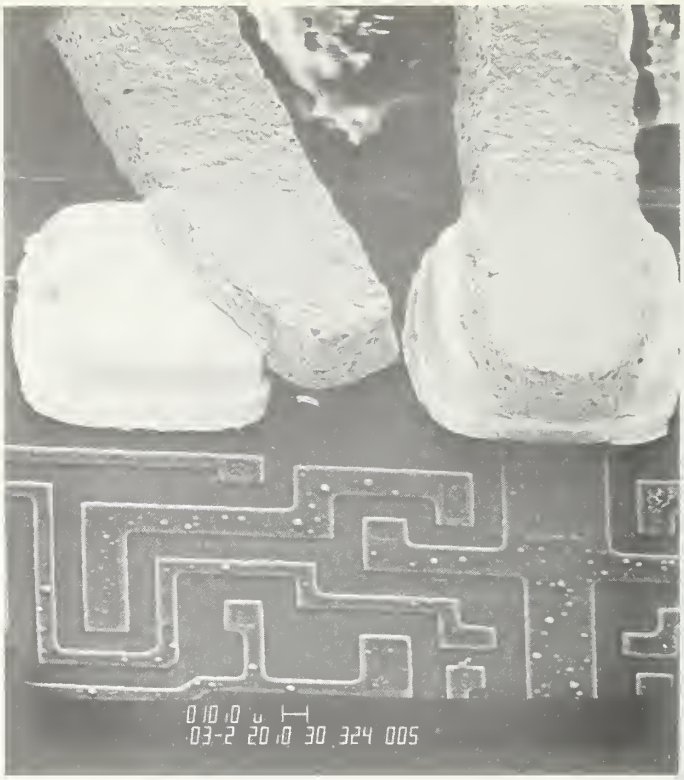

Figure 35. An SEM photograph of two bonds from a tape-bonded integrated circuit. This device, including the visually poor bond, remained intact and produced no AE even though the bonds were stressed to approximately four times the value required to produce the bond break in Figure 34.

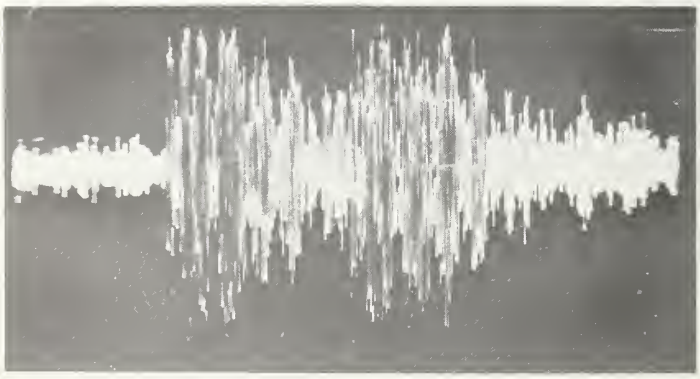

Figure 36. The acoustic emission burst from a tape-bonded lead that partially lifted at a stress of 6 gf. It gave 219 counts on an AE counter. The lead later completely lifted at 12 gf.

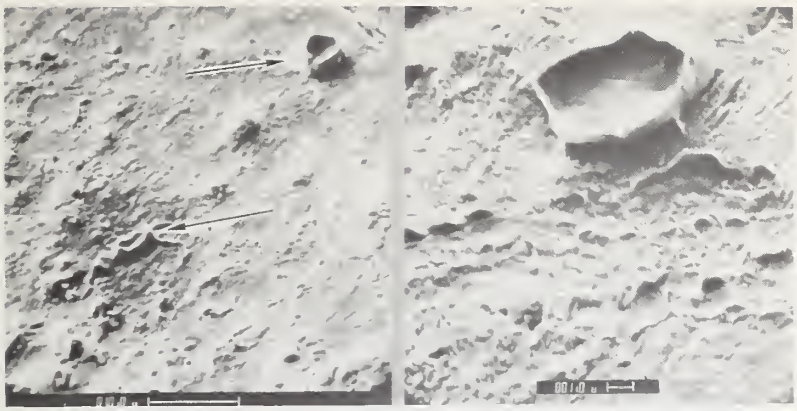

a b

Figure 37. Examples of microwelds left on the gold-plated bump from the copper tape, indicated by arrows in (a). Some of these failed by ductile "cup fracture." (b) Apparently a grain from the tape lead was left welded on the bump.

Figure 38. SEM photograph of original unstressed tape-bonded leads. The arrow on the upper lead points to the large tin-gold intermetallic compound lump. Part of the gold bump has partially dissolved in the compound. Only minimal intermetallic compound is observable on the lower lead.

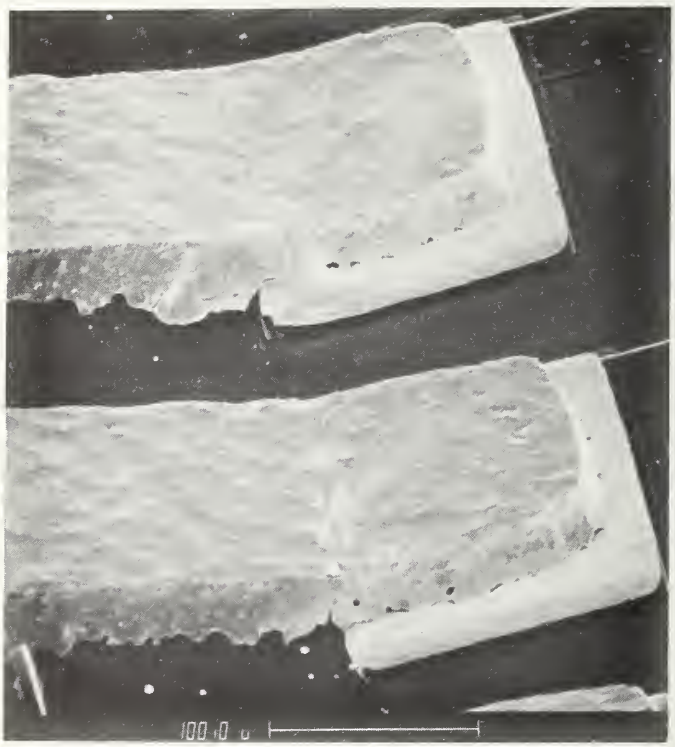

Figure 39. SEM photograph of the same two leads in Figure 38 after stressing the upper lead to 10 gf and the lower one to 7 gf. Cracks at the heel of the bond in both are obvious.

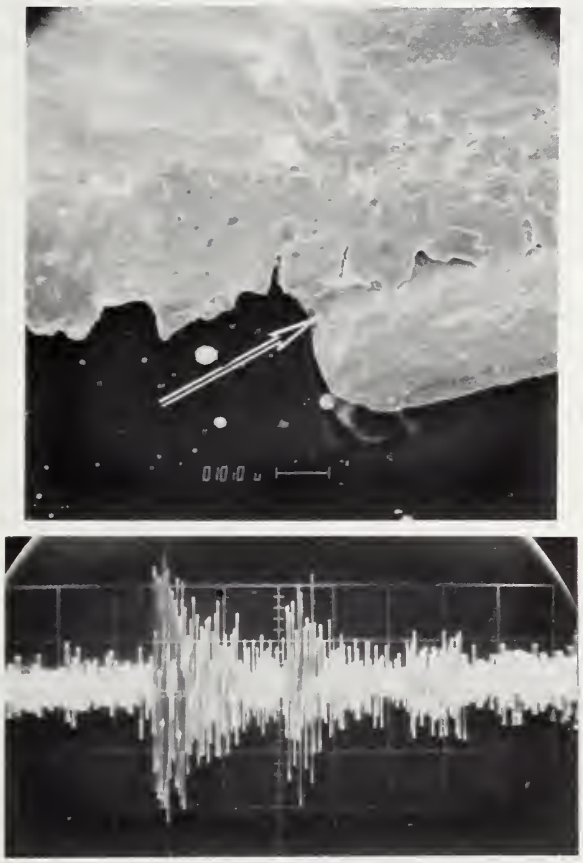

Figure 40. A close-up of the lower cracked lead and bump of Figure 39. A small amount of intermetallic compound is evident filling the area as the lead leaves the bump as shown by arrow. The double acoustic emission burst that occurred when the lead was stressed to 4 gf is shown below. The horizontal scale is 130 μs/div.

leads (and other similar ones) required 38 to 45 gf to break. Thus, for this alloyed metallurgical system, it appears that the low-stress AE, while indicative of brittle intermetallic compound formation, is not related to the ultimate bond strength of the weld.

Flip-chip devices are another area where AE may be used to verify the bond integrity. In this case visual inspection of the solder joints is almost impossible as may be seen from the SEM photograph showing a side-on view of such a flip chip in Figure 41. Therefore, it was decided to investigate the use of AE for this application. The usual method of testing for bond strength is to measure the sheer strength of the chip. This is typically in the order of 50 to 75 gf/bump for good solder joints but decreases variously to 0 for bad ones. When an AE sheer test was applied, it was found that, with rare exceptions, there were no pre-break AE bursts. Although a large burst was detected when the chip broke away, this could hardly be considered a nondestructive test. Further investigations using the stressing apparatus of Figure 23 showed that poorly soldered flip chips did emit AE when the probe was pressed down on top of the chip and orbited around. An example of a very poorly soldered chip is given in Figure 42. The weak joints were revealed by AE during downward rotating force application. The chip was then sheared off and photographed. The AE burst resulting from applying a downward force of 42 gf is shown in the lower sector of Figure 42. In numerous tests, the AE technique revealed all known poorly soldered bonds. However, the difficulty of inspecting and verifying the condition of flip chip bonds would require a long expensive study to verify that the test indeed is a reliable screen.

Various discrete components such as chip capacitors bonded into hybrids can be stressed by applying a small downward or shear force. If weakly bonded, then AE should be detectable. One such capacitor was subjected to a downward orbiting force of 200 gf. It emitted the AE signals shown in the lower portion of Figure 43. The capacitor was then broken free and photographed. Only about 15% of the intended area was actually epoxy bonded as shown by the arrows on the right side.

Since propagating cracks emit stress waves, cracks in power device chips should be detectable by current pulsing the device. Nonuniform heating of the chip during such pulses should expand the crack and cause the emission of stress waves. Cracks and flaws in hybrid substrates should also be detectable. One such cracked substrate was detected in the course of the present work while pressure testing silicone encapsulated devices. General package integrity should be assessable with AE by stressing the package under pressure or with rapid heating. Such conditions have been observed to destroy the hermeticity of potentially defective packages [5]. AE detection equipment could be used in conjunction with the nondestructive wire-bond pull-test to assist in determining the maximum nondestructive force to be applied. It could then be used to monitor that test to give ultimate assurance of its nondestructive nature. A limited evaluation of this was carried out as a preliminary to the present work and it appeared promising. Bonds that partially lifted up during a nondestructive pull were easily detected.

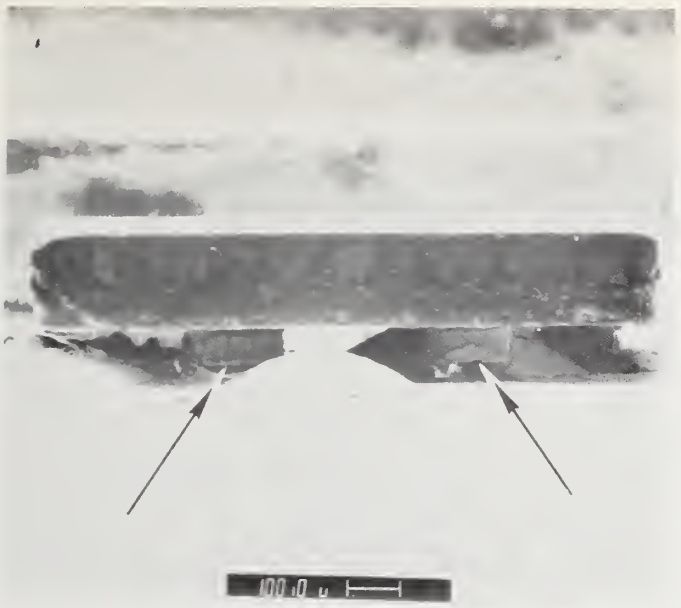

Figure 41. The SEM photograph of a side-on view of a flip-chip poorly bonded into its hybrid circuit. Arrows point to the poor solder bonds. This chip was detected by AE probing. It is almost impossible to visually inspect the bonds on flip chips.

Figure 42. A poorly soldered flip-chip shown face up beside its normal position in a hybrid microcircuit. The poor bond quality was revealed by AE, and after removing the chip, it was evident that the bumps were only partially soldered.

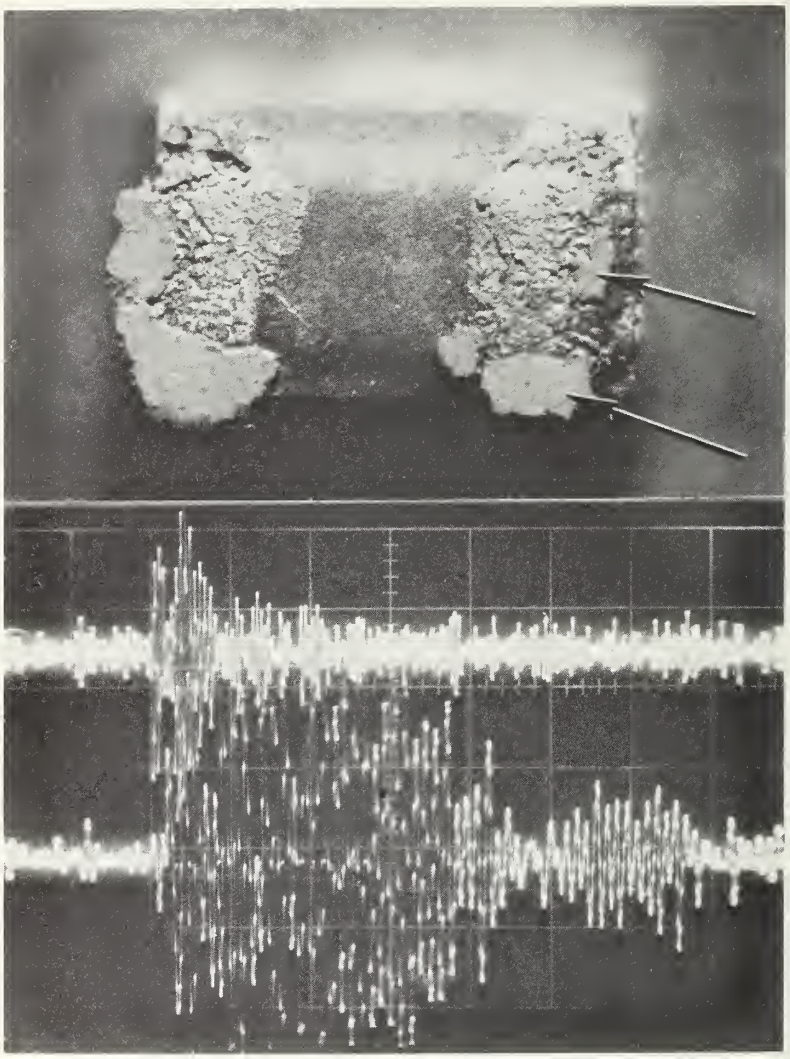

Figure 43. The upper illustration is a photomicrograph of a 2-mm long chip capacitor removed from its hybrid circuit. The arrows point to the very small areas that had been conductive-epoxy bonded to the circuit. Below is the AE waveform resulting from applying an orbiting force of 200 gf with an AE probe to the top of the capacitor before it was removed from the circuit. Both 1.1-MHz probe detector and 375-kHz substrate detector waveforms are shown. The horizontal scale is 20 μs/div.

3.5 Conclusions of Section 3

Previous studies of acoustic emission applied to real-time control or evaluation of electronics assembly processes have been reviewed. In addition, work directed towards developing AE-based tests to establish the mechanical integrity of electronics devices as screens after production are described. These studies have revealed considerable differences in the mechanical integrity of beam lead bond-anchor systems and demonstrated that AE testing offers a unique method of assessing new beam lead-nitride-anchor designs and of maintaining quality control on normal production. General deterioration of the beam-anchor system begins at pull forces of from 1.0- to 2.5-gf/beam, depending on the manufacturer. Thus, no test can be considered nondestructive that applies forces higher than about 2.0-gf/beam to the mechanically strong beam systems and perhaps 0.8-gf/beam to the weak ones. The maximum safe force for each separate manufacturing procedure must be obtained experimentally. It was found that a pull force from about 1.0 to 1.5-gf/beam was required to reveal a few poorly bonded beams in otherwise well bonded devices; however, this force is equal to the beam-system deterioration force for devices with poor mechanical integrity. For such devices, no meaningful nondestructive pull test is possible. The forces applied to the beam-anchor system for all methods of stressing, except the pull test, are dependent upon the shape of the individual beams as they extend from the chip, as well as upon the uniformity of the bugging height. Thus, to effectively use these tests, more operator care is required than is usually achieved in typical production line environments. The SR pull test is simple to employ and can be considered nondestructive if the user does not object to leaving cured SR in the package. The same material is, after all, often used as a conformal coating. The silicone resin could be applied to chips with modified epoxy die-attach equipment at either a 100% or some lower percentage sampling basis. Of the methods studied, only the SR pull test could reliably reveal weak bonds having equivalent strengths greater than 1 gf.

The main difficulty in the work with beam lead devices was encountered in the development of means of nondestructively stressing delicate, irregularly extending beam leads. However, many other uses of AE in electronics offer no such problems. Any system whose bond strength normally is destructively tested by shearing or probing, such as flip chips or capacitor chips in hybrids, can be nondestructively tested by that same method at a lower force using AE as the failure indicator. Both the inner and outer lead bonds on automated tape-bonded integrated circuits can be probed or flexed (i.e., as on a tight spool or an axial twist) while monitoring for failures with AE equipment to gain assurance that they are well bonded. The mechanical integrity of large packages can likewise be assessed by rapid heating, high or low pressure, or other means of stressing. Thus, it appears that AE will have an increasing role in assuring reliability in microelectronics.

Acknowledgment

The author gratefully acknowledges valuable discussions on hermeticity testing with S. Ruthberg and on statistical sampling with Dr. M. Natrella. The manuscript was prepared by Mrs. Kaye Dodson.

References

1. Test Methods and Procedures for Microelectronics MIL-STD-883B, November 1974.

2. Christensen, H., Electrical Contact with Thermo-Compression Bonds, *Bell Laboratories Record* 36, 127-130 (April 1958).

3. *Semiconductor Measurement Technology:* Microelectronic Ultrasonic Bonding, G. G. Harman, Ed., NBS Special Publication 400-2 (January 1974).

4. Johnson, D. R., and Chavez, E. L., Characterization of Thermosonic Wire Bonding Technique, *Proc. Intl. Microelectronics Symposium (ISHM)*, Vancouver, B.C., October 11-13, 1976, pp. 88-94.

5. Thomas, R. W., Moisture, Myth, and Microcircuits, *IEEE Trans. Parts, Hybrids, and Packaging* PHP-12, No. 3, 167-171 (1976).

6. Harman, G. G., A Metallurgical Basis for the Non-Destructive Wire-Bond Pull-Test, *Proc. 12th Annual IEEE Reliability Physics Symposium*, Las Vegas, Nevada, April 2-4, 1974, pp. 205-210.

7. Roddy, J., Spann, N., and Seese, P., Non-Destructive Bond Pull in High Reliability Applications, *IEEE Trans. Components, Hybrids and Manufacturing Technology* CHMT-1, No. 3, 228-236 (1978).

8. Ebel, G. H., Failure Analysis Techniques Applied in Resolving Hybrid Microcircuit Reliability Problems, *Proc. 15th Annual IEEE Reliability Physics Symposium*, Las Vegas, Nevada, April 12-14, 1977, pp. 70-81.

9. Shumka, A., and Piety, R. R., Migrated-Gold Resistive Shorts in Microcircuits, *Proc. 13th Annual IEEE Reliability Physics Symposium*, Las Vegas, Nevada, April 1-3, 1975, pp. 93-98.

10. Ruthberg, S., Hermetic Test Procedures and Standards for Semiconductor Electronics, *Nondestructive Testing Standards — A Review, ASTM STP 624*, Harold Berger, Ed., pp. 246-259 (American Society for Testing and Materials, 1977).

11. Harman, G. G., Metallurgical Failure Modes of Wire Bonds, *Proc. 12th Annual IEEE Reliability Physics Symposium*, Las Vegas, Nevada, April 2-4, 1974, pp. 131-141.

12. Peck, D. S., Practical Applications of Accelerated Testing, *Proc. 13th Annual IEEE Reliability Physics Symposium*, Las Vegas, Nevada, April 1-3, 1975, pp. 253-254.

13. Maximow, B., Reiss, E. M., and Kukunaris, S., Accelerated Testing of Class A CMOS Integrated Circuits, *Proc. 15th Annual IEEE Reliability Physics Symposium*, Las Vegas, Nevada, April 12-14, 1977, pp. 212-216.

14. Peck, D. S., New Concerns About Integrated Circuit Reliability, *Proc. 16th Annual IEEE Reliability Physics Symposium*, San Diego, California, April 18-20, 1978, pp. 1-6.

15. Johnson, G. M., Accelerated Test Techniques for Microcircuits, Final Technical Report MDC-E 1208, January 24, 1975, McDonnell Douglas Astronautics Co., East, Contract Report for NASA Goddard Space Flight Center.

16. Stitch, M., Johnson, G., Kirk, B., and Brauer, J., Microcircuit Accelerated Testing Using High Temperature Operating Tests, *IEEE Trans. on Reliability* R-24, No. 4, 238-250 (1975).

17. Reynolds, F. H., Accelerated Test Procedures for Semiconductor Components, *Proc. 15th Annual IEEE Reliability Physics Symposium*, Las Vegas, Nevada, April 12-14, 1977, pp. 166-178.

18. David, R. F. S., Practical Limitations of PIND Testing, *Proc. 28th IEEE Electronics Components Conference*, Anaheim, California, April 24-26, 1978, pp. 281-285.

19. Military Specifications, Microcircuits, General Specification for MIL-M-38510D, August 31, 1977.

20. Schilling, E. G., A Lot-Sensitive Sampling Plan for Compliance Testing and Acceptance Inspection, *J. Quality Technology* 10, No. 2, 47-51 (1978).

21. Joffe, A., *The Physics of Crystals*, McGraw Hill, New York, 1928.

22. Kaiser, J., Untersuchungen über das Auftreten von Geraschem Beim Zugversuch, *Arkiv für das Eisenhuttenwesen* 24, No. 1/2, 43-45 (1953).

23. Palmer, C. H., and Green, R. E., Optical Detection of Acoustic Emission Waves, *Appl. Opt.* 16, No. 9, 2333-2334 (1977).

24. Green, R. E., Acoustic Emission: A Critical Comparison Between Theory and Experiment, *Proc. Ultrasonics International Conference*, Brighton, England, June 1977.

25. Hsu, N. N., Simmons, J. A., and Hardy, S. C., An Approach to Acoustic Emission Signal Analysis Theory and Experiment, *Materials Evaluation* 35, 100-106 (October 1977).

26. Dunegan, H. L., and Harris, D. O., Acoustic Emission — A New Nondestructive Testing Tool, *Ultrasonics* 7, No. 3, 160-166 (July 1969).

27. Anderson, O. L., *The Griffith Criterion for Glass Fracture*, John Wiley & Sons, Inc., New York, 1959, and Reed-Hill, R. E., *Physical Metallurgy Principles*, second edition, D. Van Nostrand Co., New York, 1973.

28. Anderson, G. P., Bennett, S. J., and DeVries, K. L., *Analysis and Testing of Adhesive Bonds*, Academic Press, New York, 1977.

29. Green, R. E., and Pond, R. B., The Ultrasonic Detection of Fatigue Damage in Aircraft Components, Air Force Office of Scientific Res., Contract F44620-76-C-0081, March 1977.

30. Harris, D. O., Tetelman, A. S., and Darwistt, F. A., Detection of Fiber Cracking by Acoustic Emission, *Acoustic Emission, ASTM STP 505*, pp. 238-249.

31. Jon, M. C., Duncan, H. A., Vahaviolos, S. J., Analysis of Stress Wave Emission in Resistance Welding of Tantalum Capacitor, *Materials Evaluation* 36, No. 11, 40-44 (October 1978).

32. Spanner, J. C., *Acoustic Emission Techniques and Applications*, Soc. for Nondestructive Testing, 3200 Riverside Drive, Columbus, Ohio, 43221, 1974.

33. *Acoustic Emission*, ASTM Technical Publication STP 505, American Society of Testing and Materials, 1916 Race Street, Philadelphia, Pennsylvania, 1972.

34. Lord, A. E., Acoustic Emission, *Physical Acoustics*, W. P. Mason and R. N. Thurston, Eds., pp. 289-353 (Academic Press, New York, 1975).

35. Harman, G. G., The Use of Acoustic Emission in a Test for Beam Lead, TAB and Hybrid Chip Capactor Bond Integrity, *Proc. 14th Annual IEEE Reliability Physics Symposium*, Las Vegas, Nevada, April 20-22, 1976, pp. 86-97; also see *IEEE Trans. Parts, Hybrids, and Packaging* PHP-13, No. 2, 116-127 (1977).

36. Vahaviolos, S. J., Real Time Detection of Microcracks in Brittle Materials Using Stress Wave Emission, *IEEE Trans. Parts, Hybrids, and Packaging* PHP-10, No. 3, 152-159 (September 1974).

37. Saifi, M. A., and Vahaviolos, S. J., Laser Spot Welding and Real-Time Evaluation, *IEEE J. Quantum Electronics* QE-12, No. 2, 129-136 (1976).

38. Carlos, M. F., and Jon, M. C., Detection and Cracking during Rotational Soldering of a High Reliability and Voltage Ceramic Capacitor, *Proc. 28th IEEE Electronics Components Conference*, Anaheim, California, April 24-26, 1978, pp. 336-339.

39. Jon, M. C., Keskimaki, C. A., and Vahaviolos, S. J., Testing Resistance Spot Welds Using Stress Wave Emission Techniques, *Materials Evaluation* 36, No. 4, 41-51 (1978).

40. Knollman, G. C., and Weaver, J. L., Evaluation of an Acoustic Emission Monitor for On-Line Quality Control in Spotwelding of Electronic Components, *Proc. Third Acoustic Emission Symposium*, Tokyo, Japan, September 16-18, 1976, pp. 413-427.

41. Ikoma, T., Ogura, M., and Adachi, Y., Acoustic Emission From Single Crystals of Gallium Arsenide, *Ibid.*, pp. 329-341.

42. Kotani, M., Mitsui, S., and Shirahata, K., Low Noise Gunn Diode Fabrication with Consideration of a Thermocompression Bonding Effect, *Trans. IECE Japan* 58-C, 583-590 (1975).

43. Sedgwick, T., Acoustic Emission from Single Crystals of LiF and KCl, *J. Appl. Phys.* 39, 1728-1740 (1968).

44. Ikoma, T., Ogura, M., and Adachi, Y., Acoustic Emission Study of Defects in GAP-LEDS, an unpublished talk presented at the 20th Electronic Materials Conference, University of California at Santa Barbara, California, June 28-30, 1978.

45. Jellison, J. L., Effect of Surface Contamination on the Thermocompression Bondability of Gold, *IEEE Trans. Parts, Hybrids, and Packaging* PHP-11, No. 3, 206-211 (1975).

46. Holloway, P. H., and Bushmire, D. W., Detection by Auger Electron Spectroscopy and Removal by Ozonization of Photoresist Residues, *Proc. 12th Annual IEEE Reliability Physics Symposium*, Las Vegas, Nevada, April 2-4, 1974, pp. 180-186.

47. Schofield, B. H., Acoustic Emission Under Applied Stress, Technical Document Report No. ASD-TDR-63-509, Part II, pp. 1-29, May 1964, AF Materials Laboratory, Wright-Patterson AFB, Ohio.

48. Wirsing, C. E., An Ultrasonic Bond Monometallic, Gold Interconnection Technique for Integrated Packages, *Solid State Technology* 16, 48-50 (1973); also see Jellison, J. L., Kinetics of Thermocompression Bonding to Organic Contaminated Gold Surfaces, *Proc. 26th IEEE Electronics Components Conference*, San Francisco, California, April 26-28, 1976, pp. 92-97.

49. Panousis, N. T., and Bonham, H. B., Bonding Degradation in the Tantalum Nitride Chromium Gold Metallization System, *Proc. 10th Annual IEEE Reliability Physics Symposium*, Las Vegas, Nevada, April 1973, pp. 21-25.

50. Holloway, P. H., and Long, R. L., Jr., On Chemical Cleaning for Thermocompression Bonding, *IEEE Trans. Parts, Hybrids, and Packaging* PHP-11, No. 2, 83-88 (1975).

51. Tylecote, R. F., Pressure Welding of Light Alloys Without Fusion, *Trans. Institute of Welding*, pp. 163-178 (November 1946).

52. This circuit was designed and built by T. F. Leedy.

53. Dais, J. L., Mechanics of Gold-Beam-Leads During Thermocompression-Bonding, *Proc. 25th IEEE Electronics Components Conference*, Washington, DC, May 12-14, 1975, pp. 43-51.

54. Rogers, H. C., The Tensile Fracture of Ductile Metals, *Trans. Met. Soc. AIME* 218, 498-506 (1960).

NBS-114A (REV. 9-78)

U.S. DEPT. OF COMM. BIBLIOGRAPHIC DATA SHEET	1. PUBLICATION OR REPORT NO. SP 400-59	2. Gov't. Accession No.	3. Recipient's Accession No.

4. TITLE AND SUBTITLE

Semiconductor Measurement Technology: Nondestructive Tests Used to Insure the Integrity of Semiconductor Devices with Emphasis on Acoustic Emission Techniques

5. Publication Date: September 1979

6. Performing Organization Code

7. AUTHOR(S)

George G. Harman

8. Performing Organ. Report No.

9. PERFORMING ORGANIZATION NAME AND ADDRESS

NATIONAL BUREAU OF STANDARDS
DEPARTMENT OF COMMERCE
WASHINGTON, DC 20234

10. Project/Task/Work Unit No.

11. Contract/Grant No.
ARPA Order 2397

12. SPONSORING ORGANIZATION NAME AND COMPLETE ADDRESS (*Street, City, State, ZIP*)

In part by:
ARPA
1400 Wilson Boulevard
Arlington, VA 22209

13. Type of Report & Period Covered
Final

14. Sponsoring Agency Code

15. SUPPLEMENTARY NOTES

Library of Congress Catalog Card Number: 79-600131

☐ Document describes a computer program; SF-185, FIPS Software Summary, is attached.

16. ABSTRACT (*A 200-word or less factual summary of most significant information. If document includes a significant bibliography or literature survey, mention it here.*)

The discussion is divided into two major sections. The first consists of an introduction to device assembly techniques and problems followed by a review of six important nondestructive tests used during and after device packaging to insure the mechanical integrity of completed electronic devices. Most of these tests are called out in the military testing standard, MIL-STD-883 and are generally classified as screens. The first section concludes with a brief introduction to the economic and other factors that result in the choice of one screen over another and to production line statistical sampling (LTPD) appropriate to special high reliability device lots such as those used for space flight.

The second section begins with an introduction to acoustic emission, the status of theory as it can be applied to microelectronics. Then the published papers that have applied AE as a nondestructive test in electronics applications will be reviewed. Finally, passive AE techniques are applied to establishing the mechanical bond integrity of beam lead, flip chip, and tape-bonded integrated circuits as well as components in hybrid microcircuits.

17. KEY WORDS (*six to twelve entries; alphabetical order; capitalize only the first letter of the first key word unless a proper name; separated by semicolons*)

Acoustic emission; beam lead devices; electronic devices; hermeticity; hybrids; nondestructive tests; semiconductor; tape-bonded devices.

18. AVAILABILITY

☒ Unlimited

☐ For Official Distribution. Do Not Release to NTIS

☒ Order From Sup. of Doc., U.S. Government Printing Office, Washington, DC 20402, SD Stock No. SN003-003-02116-4

☐ Order From National Technical Information Service (NTIS), Springfield, VA. 22161

19. SECURITY CLASS (THIS REPORT)	21. NO. OF PRINTED PAGES
UNCLASSIFIED	72
20. SECURITY CLASS (THIS PAGE)	**22. Price**
UNCLASSIFIED	$3.50

USCOMM-DC

NBS TECHNICAL PUBLICATIONS

PERIODICALS

JOURNAL OF RESEARCH—The Journal of Research of the National Bureau of Standards reports NBS research and development in those disciplines of the physical and engineering sciences in which the Bureau is active. These include physics, chemistry, engineering, mathematics, and computer sciences. Papers cover a broad range of subjects, with major emphasis on measurement methodology, and the basic technology underlying standardization. Also included from time to time are survey articles on topics closely related to the Bureau's technical and scientific programs. As a special service to subscribers each issue contains complete citations to all recent NBS publications in NBS and non-NBS media. Issued six times a year. Annual subscription: domestic $17.00; foreign $21.25. Single copy, $3.00 domestic; $3.75 foreign.

Note: The Journal was formerly published in two sections: Section A "Physics and Chemistry" and Section B "Mathematical Sciences."

DIMENSIONS/NBS

This monthly magazine is published to inform scientists, engineers, businessmen, industry, teachers, students, and consumers of the latest advances in science and technology, with primary emphasis on the work at NBS. The magazine highlights and reviews such issues as energy research, fire protection, building technology, metric conversion, pollution abatement, health and safety, and consumer product performance. In addition, it reports the results of Bureau programs in measurement standards and techniques, properties of matter and materials, engineering standards and services, instrumentation, and automatic data processing.

Annual subscription: Domestic, $11.00; Foreign $13.75

NONPERIODICALS

Monographs—Major contributions to the technical literature on various subjects related to the Bureau's scientific and technical activities.

Handbooks—Recommended codes of engineering and industrial practice (including safety codes) developed in cooperation with interested industries, professional organizations, and regulatory bodies.

Special Publications—Include proceedings of conferences sponsored by NBS, NBS annual reports, and other special publications appropriate to this grouping such as wall charts, pocket cards, and bibliographies.

Applied Mathematics Series—Mathematical tables, manuals, and studies of special interest to physicists, engineers, chemists, biologists, mathematicians, computer programmers, and others engaged in scientific and technical work.

National Standard Reference Data Series—Provides quantitative data on the physical and chemical properties of materials, compiled from the world's literature and critically evaluated. Developed under a world-wide program coordinated by NBS. Program under authority of National Standard Data Act (Public Law 90-396).

NOTE: At present the principal publication outlet for these data is the Journal of Physical and Chemical Reference Data (JPCRD) published quarterly for NBS by the American Chemical Society (ACS) and the American Institute of Physics (AIP). Subscriptions, reprints, and supplements available from ACS, 1155 Sixteenth St. N.W., Wash., D.C. 20056.

Building Science Series—Disseminates technical information developed at the Bureau on building materials, components, systems, and whole structures. The series presents research results, test methods, and performance criteria related to the structural and environmental functions and the durability and safety characteristics of building elements and systems.

Technical Notes—Studies or reports which are complete in themselves but restrictive in their treatment of a subject. Analogous to monographs but not so comprehensive in scope or definitive in treatment of the subject area. Often serve as a vehicle for final reports of work performed at NBS under the sponsorship of other government agencies.

Voluntary Product Standards—Developed under procedures published by the Department of Commerce in Part 10, Title 15, of the Code of Federal Regulations. The purpose of the standards is to establish nationally recognized requirements for products, and to provide all concerned interests with a basis for common understanding of the characteristics of the products. NBS administers this program as a supplement to the activities of the private sector standardizing organizations.

Consumer Information Series—Practical information, based on NBS research and experience, covering areas of interest to the consumer. Easily understandable language and illustrations provide useful background knowledge for shopping in today's technological marketplace.

Order **above** *NBS publications from: Superintendent of Documents, Government Printing Office, Washington, D.C. 20402.*

Order **following** *NBS publications—NBSIR's and FIPS from the National Technical Information Services, Springfield, Va. 22161.*

Federal Information Processing Standards Publications (FIPS PUB)—Publications in this series collectively constitute the Federal Information Processing Standards Register. Register serves as the official source of information in the Federal Government regarding standards issued by NBS pursuant to the Federal Property and Administrative Services Act of 1949 as amended, Public Law 89-306 (79 Stat. 1127), and as implemented by Executive Order 11717 (38 FR 12315, dated May 11, 1973) and Part 6 of Title 15 CFR (Code of Federal Regulations).

NBS Interagency Reports (NBSIR)—A special series of interim or final reports on work performed by NBS for outside sponsors (both government and non-government). In general, initial distribution is handled by the sponsor; public distribution is by the National Technical Information Services (Springfield, Va. 22161) in paper copy or microfiche form.

BIBLIOGRAPHIC SUBSCRIPTION SERVICES

The following current-awareness and literature-survey bibliographies are issued periodically by the Bureau:

Cryogenic Data Center Current Awareness Service. A literature survey issued biweekly. Annual subscription: Domestic, $25.00; Foreign, $30.00.

Liquefied Natural Gas. A literature survey issued quarterly. Annual subscription: $20.00.

Superconducting Devices and Materials. A literature survey issued quarterly. Annual subscription: $30.00. Send subscription orders and remittances for the preceding bibliographic services to National Bureau of Standards, Cryogenic Data Center (736.00) Boulder, Colorado 80303.

U.S. DEPARTMENT OF COMMERCE
National Bureau of Standards
Washington, D.C. 20234

DFFICIAL BUSINESS

Penalty for Private Use, $300

POSTAGE AND FEES PAID
U.S. DEPARTMENT OF COMMERCE
COM-215

SPECIAL FOURTH-CLASS RATE
BOOK